CHALMERS
UNIVERSITY OF TECHNOLOGY

Investigations of Bi-phasic Drug Depletion in Liver Microsomes and Hepatocytes in Metabolic Stability Studies

Master of Science Thesis

MADELEINE ENGSEVI

Department of Chemical and Biological Engineering
CHALMERS UNIVERSITY OF TECHNOLOGY
Gothenburg, Sweden 2015

Investigations of Bi-phasic Drug Depletion in Liver Microsomes and Hepatocytes in Metabolic Stability Studies

Master of Science Thesis

Madeleine Engsevi

Investigations of Bi-phasic Drug Depletion in Liver Microsomes and Hepatocytes in Metabolic Stability Studies

Madeleine Engsevi

Department of Chemical and Biological Engineering
Chalmers University of Technology
SE - 412 96 Göteborg
Sweden

This thesis was performed at Discovery Sciences, AstraZeneca, Mölndal under the supervision of Senior Research Scientist Anna Novén.

[Chalmers Reproservice]

Göteborg, Sweden 2015

Acknowledgement

First I would like to give special thanks to my supervisor Anna Novén for great support and dedication at all times, also for the long discussions, sharing of useful knowledge and answering any type of question at any time. I would also like to thank team leader Erika Rehnström for great encouragement and support during the whole process of my project.

Many thanks to Pär Nordell for enthusiastically helping me with the modelling work and sharing his knowledge and to Susanne Winiwarter for helping with the *in vivo* predictions and interpretations of the results. Special thanks to Johan Hulthe for technical support with the robots and templates at any time.

Finally, many thanks to all the colleagues at AstraZeneca, Mölndal, for helping me finding my way around and feeling welcome.

Abstract

Development of a new drug is a long and costly process and to avoid attritions due to inadequate metabolic and pharmacokinetic data it is important to determine these early by the use of *in vitro* systems. The intrinsic clearance (CL_{int}) is calculated from the disappearance of test compound in the incubation plate over time and for most compounds this disappearance is linear, however, some compounds show a bi-phasic depletion profile which can cause under predictions of *in vivo* clearance when using the same calculation model. To improve the quality of the assay for these compounds the reasons behind the bi-phasic depletion profile were investigated. A set of 26 carboxylic acids were incubated with rat hepatocytes and human liver microsomes (HLM) on robot and the disappearance was determined by LC-MSMS on HSS T3, CSH and BEH C18 columns. The incubations with HLM suggest that conjugative metabolism dominated for this set of compounds. Viability and matrix matched zero time point had no impact on the depletion curve. Mass/chromatographic interferences from co-elution of metabolites were observed for two of the compounds which likely had an impact on the response but this could not explain the bi-phasic profile. The identities of the hydroxy and acyl glucuronide metabolites were confirmed on quadrupole time-of-flight (Q-TOF). A correlation was found between high $LogD_{7.4}$ and a more bi-phasic appearance at higher cell concentrations. The depletion was modelled with a bi-exponential model that produced unbiased CL_{int} values that were less prone to cause under prediction of *in vivo* clearance.

Keywords: Metabolic stability, intrinsic clearance, bi-phasic depletion, rat hepatocytes, human liver microsomes

Table of Contents

1. Introduction 1
1.1. Phase I and II Metabolism 1
1.2. In Vitro Systems 2
1.3. Intrinsic Clearance 3
1.4. Factors that may impact the depletion curves 6
1.5. Project Aim 8
3. Methods 9
3.1. Equipment, Materials and Reagents 9
3.2. Selection and Preparation of Test Compounds 10
3.3. Preparation of the Incubation Mixtures 11
3.3.1. Preparation of Hepatocytes 11
3.3.2. Preparation of Microsomal Suspension 12
3.4. Preparation of “True Zero” 12
3.5. Metabolic Incubations on the Robot 13
3.6. Determination of Hepatocyte Viability after Incubation 13
3.7. Liquid Chromatography Tandem Mass Spectrometry Analysis 13
3.7.1. Calculations 14
3.8. Data Modelling for Determining CL_{int} 15
3.9. Metabolite Identification 16
4. Results and Discussion 17
4.1. Measurement of Viability during Incubation 17
4.2. Chromatographic and Mass Interferences 18
4.3. Impact of Protein Concentration on the Depletion Curve 22
4.4. Confirmation of Metabolite Identity 25
4.5. Data Modelling for Objective Calculations of CL_{int} 29
4.6. Impact of Choice of Model on the Predictions of in vivo Clearance 32
4.7. Assessment of the Importance of True Zero 34
5. Conclusions 37

6. Future Studies 39
7. Bibliography 40
8. Appendix I 43

1. Introduction

The development of a new drug is a long and costly process involving many steps starting with target identification and screening, followed by lead generation and optimization and finally pre-clinical and clinical trials before the drug can be registered and launched on the market (Bleicher, Böhm et al. 2003). In 2002 the average cost for developing a new drug was approximately 900 million USD and the average development time 12 years (Kola and Landis 2004). In 1991, inadequate metabolic and pharmacokinetic data was the reason for 40% of the attritions by the US Food and Drug Administration (FDA) and so pharmaceutical companies have invested in additional approaches to increase the success rate for new drugs, such as the increased use of *in vitro* systems (Thompson 2001, Baranczewski, Stanczak et al. 2006). Determination of the metabolic profile, along with lipophilicity, solubility and protein binding, early in the discovery process can either be used to modify the compound to obtain more favourable metabolic properties, or to discard the compound early (Plant 2004). For example, a compound that is rapidly metabolised may not have satisfactory bioavailability *in vivo* (Baranczewski, Stanczak et al. 2006). This approach has proven both time and cost effective and had reduced the attritions for inadequate metabolic data to 10% by year 2000 (Kola and Landis 2004).

1.1. Phase I and II Metabolism

The physical property that allows the drug, or any xenobiotic, to be absorbed through the gastrointestinal tract, skin or lungs, is the lipophilicity. Due to this, the elimination process by a series of enzyme catalysed metabolism reactions is usually a conversion from lipophilicity, which favours absorption, to hydrophilicity, which favours excretion through urine and bile (Crespi 1995, Parkinson 2001, Thompson 2001). Generally the metabolism of the drug can be divided into two phases; phase I and phase II. During phase I, the compound undergoes oxidation, hydrolysis and reduction reactions catalysed by a number of enzymes such as cytochrome P450 (CYPs) and flavin-containing monooxygenases (FMOs) (Hasler, Estabrook et al. 1999, Rendic 2002). Phase II involves conjugation reactions of lipophilic compounds catalysed by enzymes like UDP-glucuronosyltransferase (UGTs) and sulfotransferases (STs) with cofactors uridine diphosphate-glucuronic acid and 3'phosphoadenosine-5'-phosphosulfate respectively (Chiu 1993, Tukey and Strassburg 2000, Parkinson 2001). Not all compounds go through both these phases of metabolism, some compounds are

metabolised purely by phase II reactions. However, after any of these reactions the compound is more hydrophilic and more easily eliminated from the body (Parkinson 2001).

1.2. In Vitro Systems

Two *in vitro* systems widely used in metabolic research are microsomes and hepatocytes. Microsomes are vesicles that consist of endoplasmic reticulum and therefore contain mostly CYP and UGT enzymes (Brandon, Raap et al. 2003). These are prepared by ultracentrifugation from human and animal tissues, usually the liver tissue (Clarke 1998), and to achieve a standard enzyme concentration without individual variation, samples from different donors are often pooled (Taavitsainen, Juvonen et al. 2001, Brandon, Raap et al. 2003). The enzyme activity of microsomes can be preserved for extended durations through storage in a freezer, but for the enzymes to be active after defrosting, co-factors have to be added to the suspension (Venkatakrishnan, von Moltke et al. 2003). The microsome system makes it possible to distinguish between the activity of different enzymes like glucuronosyltransferase (UGT), flavin-containing monooxygenase (FMO) and Cytochrome P450 (CYP). This model is well used for prediction of *in vivo* clearance, although the enzyme activity decreases after two hours, and thus place a limit on the incubation time (Baranczewski, Stanczak et al. 2006).

Another *in vitro* model that is even closer to the *in vivo* conditions is the hepatocyte. This model contains both phase I and phase II enzymes as well as the necessary co-factors, which make it suitable for estimation and prediction of hepatic clearance along with other properties such as drug-drug interactions (Hewitt, Gómez Lechón et al. 2007). A disadvantage with fresh human hepatocytes is the limited availability and the rapid decrease in viability, which make it necessary to cultivate them immediately after isolation and use them within days (Brandon, Raap et al. 2003). Through cryopreservation of the hepatocytes these problems can be mitigated, and if thawed correctly, the enzymatic activity can be comparable to the activity of the fresh hepatocytes with a decrease of only 10-20% (Baranczewski, Stanczak et al. 2006).

1.3. Intrinsic Clearance

The metabolic stability of a compound is determined by the amount of compound that is metabolised during incubation with cells, or cell fractions, over a period of time and is expressed as intrinsic clearance (CL_{int}) and *in vitro* half-life ($t_{1/2}$) (Venkatakrishnan, von Moltke et al. 2003). This process can be automated through the use of robots, which enables testing of a large set of compounds, and is widely used within discovery drug metabolism and pharmacokinetics (DMPK) (Jenkins, Angeles et al. 2004, Riley and Grime 2004). Based on these values, parameters like bioavailability, *in vivo* clearance and hepatic clearance (CL_H) can be calculated. To correctly interpret the metabolic stability assay, a number of assumptions have to be made, such as the liver being the major organ for clearance of the test compound, and that the major elimination pathway is oxidative metabolism. Furthermore, the *in vitro* rate of the enzymes is the same as *in vivo*, the concentration of the test compound is below the Michaelis-Menten constant (K_m), and that there is no inactivation of the enzymes. Finally, it is assumed that there is no non-specific protein binding of the test compound (Baranczewski, Stanczak et al. 2006).

The clearance of a compound from a "well stirred" model can normally be described by first order reactions which produce an exponential decay type curve. The equation for the decay and the more applicable logarithmic version of the equation are as follows:

$$y(t) = y(0) \cdot exp(-kt)$$

$$\ln y(t) = \ln y(0) - kt$$

where y(t) is the concentration of the compound at time t, y(0) is the initial concentration of the component, and k is the rate of decay of the component. From k the CL_{int} is calculated:

Microsomes:

$$CL_{int} = k\ (min^{-1})\ \frac{V_{incubation}\ (\mu l)}{P_{incubation}(mg)} \qquad (\mu l/[min \cdot mg])$$

Hepatocytes:

$$CL_{int} = k\ (min^{-1})\ \frac{V_{incubation}\ (\mu l)}{N_{number\ of\ cells}(10^6)} \quad (\mu l/[min \cdot 10^6])$$

where V is the incubation volume, P is the amount of protein and N is the number of cells. From the rate of decay the half-life ($t_{1/2}$) of the compound can also be calculated:

$$t_{1/2} = ln2/k$$

where k is determined experimentally from the slope of the logarithmic first order reaction as described above. A typical example of that can be seen in Figure 1.

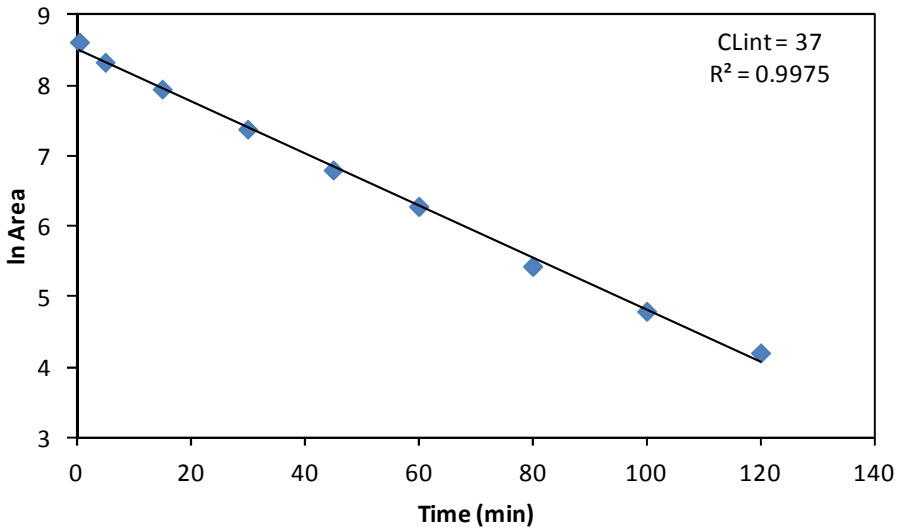

Figure 1. A typical example of a linear depletion as exhibited by most compounds. A linear regression is fit to the data points with a good fit and the CL_{int} is calculated to be 37 µl/[min·10^6].

However, not all compounds follow this depletion model. As shown in Figure 2, some compounds exhibit a bi-phasic depletion curve where the curve displays two linear regions, and a single regression will result in a poor fit to the data. As CL_{int} is defined as "the maximum activity of the liver towards a drug, in the absence of other physiological determinants such as hepatic blood flow and drug binding within the matrix" (Baranczewski, Stanczak et al. 2006), the CL_{int} calculated in Figure 2a might be an underestimation and could lead to an under prediction of the *in vivo* clearance. The calculation of CL_{int} with the initial

high gradient, as shown in Figure 2b, may be closer to the true value, although this evaluation method is subjective.

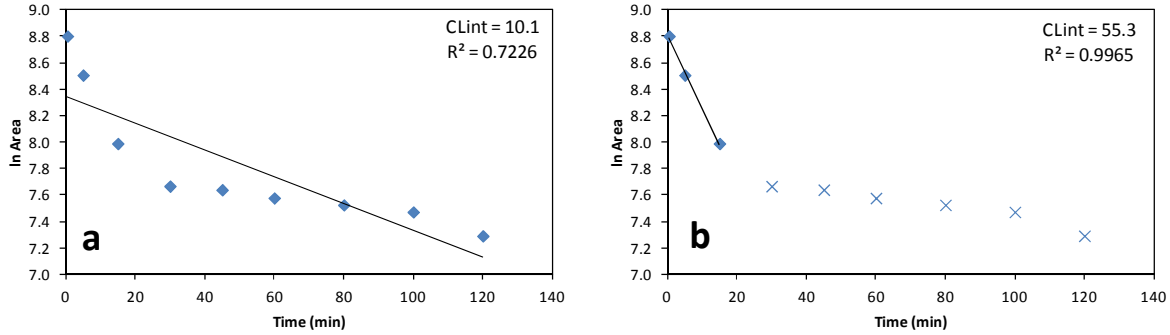

Figure 2. An example of a compound with a bi-phasic depletion profile with the CL_{int} calculated using a) all data points and b) only the first phase. Using all data points results in a poor fit and a calculated CL_{int} of 10.1 µl/[min·10^6], compared to a value of 55.3 µl/[min·10^6] using only the first phase, which has a good linear fit, but is subjective and prone to errors.

A problem associated with *in vivo* clearance predictions from *in vitro* data is a systematic under prediction (Hallifax, Foster et al. 2010). To avoid this systematic bias, the values are corrected using a regression line generated from *in vivo* clearance data and scaled *in vitro* intrinsic clearance from incubations of isolated hepatocytes. The reference compounds used in making this regression line were selected for their route of elimination being primarily metabolic clearance (Sohlenius-Sternbeck, Jones et al. 2012). The *in vitro in vivo* extrapolation (IVIVE) can be visualised by plotting *in vivo* CL_{int} values against corrected predicted *in vivo* CL_{int} values (Wilson, Rostami-Hodjegan et al. 2003), and with an accurate IVIVE the *in vitro* CL_{int} can be used for efficient drug design. A study performed by Sohlenius-Sternbeck et al. showed that when the regression line was applied to the data, 66% of the compounds had a predicted *in vivo* CL_{int} within a two-fold of the derived *in vivo* CL_{int} for humans, and the same number was 54% in rat (Sohlenius-Sternbeck, Jones et al. 2012). For CL_{int} values calculated from bi-phasic depletion curves there is a risk of under-prediction, especially due to the subjectivity of the method and it is therefore important to use an objective model for the calculation of CL_{int}. Alternative ways of calculating CL_{int} values along with the impact on the *in vivo* clearance were investigated in this project.

1.4. Factors that may impact the depletion curves

Improved understanding of the bi-phasic profiles and their interpretation is necessary for further assay development, and will subsequently lead to improved data quality enabling more accurate predictions of *in vivo* hepatic clearance. The drug depletion method makes the assumption that the concentration of the drug in the surrounding medium and in the cell is the same, although this may not be the case due to transporter protein activity. To distinguish between the hepatic uptake clearance and the hepatic metabolic clearance, Jigorel and Houston compared the results from the conventional method and a media-loss experiment (Jigorel and Houston 2012). It was found that for some of the tested compounds, including Atorvastatin, the media-loss experiment showed a bi-phasic decay whereas the conventional method showed a linear depletion of the compound. The authors concluded that this was likely due to an uptake rate faster than metabolism, which resulted in the accumulation of the compounds inside the cells (Jigorel and Houston 2012).

Studies by Jones and Houston found that enzyme instability during incubation may cause a bi-phasic depletion of the test compound (Jones and Houston 2004). Another phenomenon that could have an impact on the kinetics of the metabolism is nonspecific binding of the compound to the membranes, which in turn could have an impact on the *in vivo* clearance prediction (Austin, Barton et al. 2005). In general, the free fraction of the compound in the incubation mixtures is assumed to be the same as the total amount of compound. This assumption is used for the calculations of the metabolic parameters K_m and K_i and is unlikely to be the case for an *in vitro* situation (Obach 1999). Because of this, the unbound intrinsic clearance ($CL_{int,U}$) and the CL_{int} are not the same for many compounds. Previous studies in microsomes have shown that some compounds have a high binding to microsomes and consequently, protein concentration can have an impact on the *in vivo* prediction (Kalvass, Tess et al. 2001, Austin, Barton et al. 2002). Studies have shown that the binding to hepatocytes is a passive process where equilibrium is reached rapidly, and the extent of hepatocyte binding is increased in compounds with higher lipophilicity (Ichinose and Kurihara 1985). A study by Austin et al. also observed a realationship between the lipophilicity of the compound and the nonspecific binding to hepatocytes through a comparison of $LogD_{7.4}$, the octanol-water partition coefficient at pH 7.4 (Smith, Jones et al. 1996). They found that compounds with high $LogD_{7.4}$ values were more prone to unspecific binding to hydrophobic compartments such as the phospholipids of the cell membranes, and

in addition, this non-specific binding has been shown to be independant of cell viability (Austin, Barton et al. 2005). It has been shown by Obach that in general, acidic compounds bind to plasma proteins, but only bind to a negligible extent to human liver microsomes (Obach 1999). For neutral and basic compounds, the extent of binding is the same in the *in vivo* and *in vitro* systems and should also be included in the predictive model.

During incubation, the test compound is metabolised into unknown metabolites and the column selection for chromatographic analysis is important for data quality and can have an impact on the final results based on the measurement of the peak area for the test compound. If the wrong column is chosen, then co-elution of metabolites and the test compound can occur, which can result in a suppressed or enhanced signal and consequently the peak area could be over- or underestimated. In addition, the matrix of the sample could have a considerable impact on the results and can have an effect on factors such as limit of detection, limit of quantification, accuracy, precision, linearity and therefore also reproducibility. Although this phenomenon is not fully understood, one reason is probably co-elution of compounds on the analyte ionisation. The chemical nature of the analyte is of importance for the matrix effect (ME), however, these effects may be reduced by improving the liquid chromatography separation (Trufelli, Palma et al. 2011).

One occurrence that could have an impact on the appearance of the depletion curves, and hence the calculated CL_{int} values, could be inadequate chromatographic separation that results in the co-elution of acyl glucuronides. Loss of the glucuronide moiety (176 Da) from the acyl glucuronide in the ion source converts the metabolite back into the test compound. If the chromatographic separation is poor between the test compound and its acyl glucuronide, the signal of the test compound will be overestimated due to the contribution from mass interference caused by the ion-source conversion of acyl glucuronide (Xue, Akinsanya et al. 2008). An example of this fragmentation is shown for Atorvastatin and the corresponding acyl glucuronide in Figure 3.

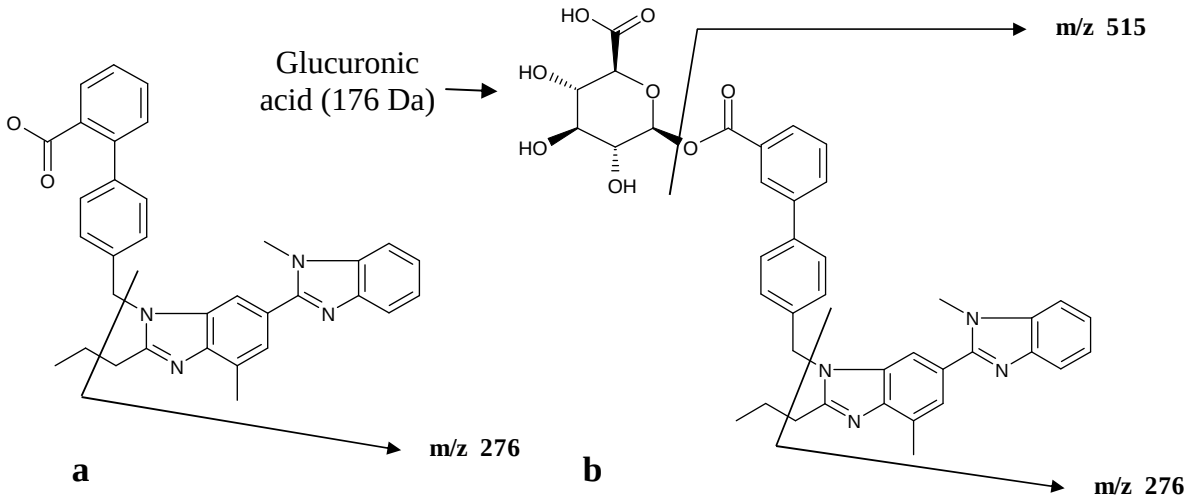

Figure 3. Fragmentations of a) Atorvastatin and b) Atorvastatin acyl glucuronide. Note that the loss of dehydrated glucuronic acid (176 Da) converts the compound back to Atorvastatin.

1.5. Project Aim

The aim of the project was to investigate the bi-phasic nature of drug depletion in rat hepatocytes and human microsomes of a set of compounds with respect to experimental conditions, analytical set up and calculation approach as a means to improve the quality of the assay for these compounds.

3. Methods

This section contains a list of the equipment, materials, chemicals and reagents that were used for the experiments along with a description of how the samples were prepared. In addition, the analysis technique with LC-MSMS is described as well as the data processing and modelling work for calculation of CL_{int}.

3.1. Equipment, Materials and Reagents

This section briefly lists the technical equipment, materials and chemicals used for the preparation of the samples that were analysed by LC-MSMS.

Equipment

Tecan Freedom Evo 200 robot (Tecan, Switzerland) with plate shaker Variomag Teleshake 70 with TEC Control 485 (Thermo scientific, United States), Agilent Bravo Automated Liquid handling Platform (Aglient Technologies, United States), Eppendorf Centrifuge 5810R (Eppendorf, Germany), Casy Innovatis cell counter (Roche Innovatis AG, Germany).

Materials

NUNC 1 ml 96-deepWell PP Plate Natural (260252, Thermo scientific), conical NUNC plates 0.45 ml/well (249944, Thermo Scientific), Microwell lid (263339, Thermo Scientific), NUNC 96 well cap natural (276002, Thermo Scientific), Cryopreserved male hepatocytes Rat Han Wistar obtained from Bioreclamation IVT, lot no. COA, Human liver microsomes supplied by BD Gentest UltraPool 150 donor (Lot No.38289) (Products and Services, United States).

Chemicals and Reagents

Acetonitrile (ACN) of HPLC grade (*e.g.* Rathburn, Scotland), formic acid of *p.a.* quality (*e.g.* Merck, Germany), water of *e.g.* Elga quality (Elga Ltd, England), L-15 Leibovitz buffer (Gibco 21083-027), 5,5-Diethyl-1,3-diphenyl-2-iminobarbituric acid (no.39): Molecular weight 321.4 g/mol (Sigma-Aldrich, Sweden), Dimethyl Sulphoxide (DMSO) 78,13 g/mol (Sigma-Aldrich D2650), Casyton 05 651 808 001 (Roche, Switzerland), potassium dihydrogen phosphate of *p.a.* quality (*e.g.* Sigma-Aldrich), di-sodium hydrogen phosphate of

p.a. quality (*e.g.* Merck, Germany), ß-nicotinamide adenine di-nucleotide phosphate, reduced form (ß-NADPH) (Sigma Chemical, USA).

Test compounds stock solution: 2 µl of 10 mM solution of test compounds was delivered from the internal Compound Management, Mölndal in 96 well plate in pure DMSO.

Stop solution: 0.2 ml of 1 mM no.39 stock solution acid was added to 1000 ml of acetonitrile and 8 ml pure formic acid. This solution was stored at 4 °C.

Phosphate buffer (pH=7.4): 100 mM Na_2HPO_4 buffered with about 30 ml of 100 mM KH_2PO_4.

3.2. Selection and Preparation of Test Compounds

A retrospective review of data previously obtained from metabolic stability in hepatocytes showed that bi-phasic nature was predominantly exhibited by carboxylic acids; so for this reason only carboxylic acids were chosen for this investigation. Out of the test compounds, nine were commercial pharmaceutical compounds that are either available or have been withdrawn from the market, while the other seventeen were compounds from Astra Zeneca's compound collection. In addition to the twenty six test compounds six control compounds were included to ensure the quality of the assay and results.

The stock solution of the test compounds was delivered by Compound Management, Mölndal, Sweden in a 96 well plate. Four identical plates contained 2 µl of 10 mM in DMSO for 26 test compounds and 6 control compounds and three of these plates were used to prepare the 50 µM test solution plate (Figure 4a). The test compound stock solution plates were diluted in 98 µl in a 50% ACN solution by Bravo automated liquid handler. An aliquot of 40 µl from each of the wells of the three plates of the diluted test compound stock solution was added to 120 µl 50% ACN solution in the same plate creating triplicates for each compound at a 50 µM concentration (Figure 4b).

a

	1	2	3	4	5	6	7	8	9	10	11	12
A	cpd1	cpd9	cpd17	cpd25								
B	cpd2	cpd10	cpd18	cpd26								
C	cpd3	cpd11	cpd19	cpd27								
D	cpd4	cpd12	cpd20	cpd28								
E	cpd5	cpd13	cpd21	cpd29								
F	cpd6	cpd14	cpd22	cpd30								
G	cpd7	cpd15	cpd23	cpd31								
H	cpd8	cpd16	cpd24	cpd32								

b

	1	2	3	4	5	6	7	8	9	10	11	12
A	cpd1	cpd9	cpd17	cpd25	cpd1	cpd9	cpd17	cpd25	cpd1	cpd9	cpd17	cpd25
B	cpd2	cpd10	cpd18	cpd26	cpd2	cpd10	cpd18	cpd26	cpd2	cpd10	cpd18	cpd26
C	cpd3	cpd11	cpd19	cpd27	cpd3	cpd11	cpd19	cpd27	cpd3	cpd11	cpd19	cpd27
D	cpd4	cpd12	cpd20	cpd28	cpd4	cpd12	cpd20	cpd28	cpd4	cpd12	cpd20	cpd28
E	cpd5	cpd13	cpd21	cpd29	cpd5	cpd13	cpd21	cpd29	cpd5	cpd13	cpd21	cpd29
F	cpd6	cpd14	cpd22	cpd30	cpd6	cpd14	cpd22	cpd30	cpd6	cpd14	cpd22	cpd30
G	cpd7	cpd15	cpd23	cpd31	cpd7	cpd15	cpd23	cpd31	cpd7	cpd15	cpd23	cpd31
H	cpd8	cpd16	cpd24	cpd32	cpd8	cpd16	cpd24	cpd32	cpd8	cpd16	cpd24	cpd32

Figure 4. a) The design of the 10 mM stock solution of test compound plate and b) design of the 50 µM test solution plate.

3.3. Preparation of the Incubation Mixtures

The following experiments were performed using either rat hepatocytes or human liver microsomes; with the relevant preparation description for each compound described below.

3.3.1. Preparation of Hepatocytes

Rat Han Wistar cryopreserved hepatocytes (COA) from storage at -150°C were transported, covered in dry ice, and thawed in a water bath at 37°C until the hepatocytes detached from the vials. The suspension was then transferred to falcon tubes containing 45 ml of Leibovitz L-15 buffer and centrifuged at 50g for 3 min at room temperature. The supernatant was discarded and the washing step was repeated. The pellet was re-suspended in Leibovitz buffer and the cell suspension diluted to a concentration of approximately 3 million cells/ml.

An aliquot of 25 µl of the cell suspension was added to 10 ml of Casyton and the cell count and cell viability was determined using CASY Innovativs cell counter. Three dilutions of the cell suspension were prepared (0.25, 1, and 2 million cells/ml) and 245 µl of the dilutions were dispensed into a 1 ml round bottom 96 well Nunc plate, 32 wells for each cell

concentration. The blank plate was prepared with 15 µl of the cell dilutions, 32 wells for each cell concentration. The incubation plate was then loaded onto the Tecan Freedom Evo 200 robot.

3.3.2. Preparation of Microsomal Suspension

Human liver microsomes (BD38289, 20 mg/ml protein concentration) from storage at -80°C were thawed in a water bath at 37°C. A 20 mM NADPH solution was prepared by dissolving 54 mg of NADPH in 3.2 ml of phosphate buffer (pH = 7.4). Three different protein concentrations were prepared (0.27, 1.1, and 2.2 mg/ml) by mixing the protein suspension (187.5, 750, and 1500 µl) with an equal volume of 20 mM NADPH solution before the addition of phosphate buffer (pH = 7.4) to a total volume of 13.5 ml.

The three microsomal mixtures were dispensed in a 1 ml round bottom 96 well Nunc plate, 32 wells for each protein concentration, 245 µl per well. The blank plate was prepared with 15 µl of the cell dilutions, 32 wells for each cell concentration. The incubation plate was then loaded onto the Tecan Freedom Evo 200 robot.

3.4. Preparation of “True Zero”

For preparation of the true zero the hepatocytes were thawed, washed and diluted in the same way as in the cell preparation mentioned in 3.3.1. The cells were quenched by adding 3 ml of cell suspension to 18 ml of stop solution (ACN, 0.8% F.A, 100 nM 5,5-Diethyl-1,3-diphenyl-2-iminobarbituric acid (no.39) as internal standard) in falcon tubes, one for each cell concentration. The tubes were centrifuged at 4000 rpm for 20 min at 4°C. The plate containing the extracted cell suspension was prepared by dispensing 245 µl of supernatant into a 1 ml round bottom 96 well Nunc plate, 32 wells for each supernatant and the plate was loaded onto the Tecan Freedom Evo 200 robot.

A 5 µl aliquot of the 50 µM test solution was added to the plate, containing 245 µl of extracted matrix, by the robot and after mixing, a 15 µl sample of the mixture was added to a stop plate prepared with 90 µl of extracted matrix. The stop plate was centrifuged at 4000 rpm for 5 min at 4°C and then 50 µl of the supernatant was diluted in 50 µl of extra pure Elga

water by Tecan Freedom Evo-2 200. The plate was sealed with a microwell lid was then stored at 4°C.

3.5. Metabolic Incubations on the Robot

The incubation plate was pre-incubated for 15 min at 37°C on the Tecan Freedom Evo 200 robot with a Variomag Teleshake 70 at 13 Hz, where the temperature and shaking frequency was kept throughout the incubation. After pre-incubation, 5 µl of the 50 µM test solution was added to the incubation plate by the robot. The final concentration of the test compound in the incubation mixture was µM and the content of organic solvents was 1% ACN and 0.01% DMSO. At each time point (0.5, 5, 15, 20, 30, 45, 60, 80, 100 and 120 min) an aliquot of 15 µl was taken and quenched in 90 µl of stop solution at 4°C. The quenched plates (one for each time point) were centrifuged at 4000 rpm for 20 min at 4°C and then 50 µl of the supernatant was diluted in 50 µl of extra pure Elga water by Tecan Freedom Evo-2 200. The plates were sealed with microwell lids and stored at 4°C until LC-MSMS analysis.

3.6. Determination of Hepatocyte Viability after Incubation

The remainder of the hepatocytes solution (3 million cells/ml, described in Section 3.3.1) was dispensed in triplicates of 245 µl in each well to a 1 ml round bottom 96 well Nunc plate. This plate was loaded onto the robot during the metabolic experiments (Section 3.6) and underwent the same 37°C incubation and 13 Hz shaking for the full duration of the experiment (120 min), after which the viability of the cells in the three wells was measured using the CASY Innovatis cell counter as described above. The remainder of the cell suspension was placed in the 37°C water bath during the time of incubation and the viability was measured after one and two hours.

3.7. Liquid Chromatography Tandem Mass Spectrometry Analysis

The samples were analysed with ultra-performance liquid chromatography and tandem mass spectrometry with ESI (UPLC-MS/MS) (Waters ACQUITY TQD) assisted with column manger using three different ACQUITY UPLC columns: HSS T3, CSH and BEH C18, each with dimensions of 2.1x30 mm and packed with 1.7 µm diameter particles. The chromatography was performed with a 5 µl injection volume at a flow rate of 1.0 ml/min with

a short gradient elution. The mobile phases consisted of A (water with 0.1% formic acid) and B (Acetonitrile with 0.1% formic acid). The elution profile was as follows: 0.2% B for the first 0.1 minutes, then a linear increase to 95% B at 0.7 minutes, holding at 95% until the 1.0 minute mark, then a linear decrease back to 0.2% ending at 1.1 minutes. Detection was achieved by the multiple reactions monitoring of the transitions determined in optimization process by using MassLynx (Waters). The thermally labile glucuronides were expected in the same transitions as the test compounds if the chromatographic separation was achieved. The hydroxy metabolites were detected using semi single reaction monitoring data acquisition. Acquired data was processed using TargetLynx (Waters) and each peak was inspected before the data was exported into the Excel (Microsoft) calculation template.

3.7.1. Calculations

The depletion curve was visualised by plotting the natural logarithm of the peak area against time. A line was then fit to the data and if the slope of the line significantly differed from zero, a statistical analysis of the depletion curve was performed. In principal, a significant correlation between concentration and time was obtained when the absolute t-value of the depletion coefficient was higher than the critical t-value, t_{α}. The t-value was calculated as follows:

$$t = \frac{r}{\sqrt{(1 - r^2)/(n - 2)}}$$

Where 'r' is the correlation coefficient and 'n' is the number of data points. In the Excel template the critical t-value (t_{α}) is calculated as TINV(α; n-2), where the t-statistic (α) was set to 0.05, which corresponds to a 95% confidence in the result.

The graphs were then visually inspected. For the compounds with a linear depletion curve and a passed t-test a single CL_{int} value was calculated. For the compounds with a bi-phasic depletion curve two values were calculated; one based on all time points and a past t-test and one based on the steeper slope of the curve and a passed t-test. The CL_{int} values were then normalised against cell concentration and used in a prediction model to predict *in vivo* clearance.

3.8. Data Modelling for Determining CL_{int}

As an attempt to better model the bi-phasic depletion curves, a bi-exponential equation was also fitted to the data in addition to the standard mono-exponential equation. The two models were as follows:

Mono-exponential model:

$$y(t) = A \cdot e^{-Bt}$$

Bi-exponential model:

$$y(t) = A \cdot e^{-Bt} + C \cdot e^{-Dt}$$

where the parameters A, B, C and D are the fitted parameters. As the bi-exponential model has two rates of decay, B and D, a single value was found from the formula:

$$A^* = \frac{AB + CD}{A + C}\Big|_{bi-exponential}$$

where A* is a single rate of clearance that has the same initial gradient as the bi-exponential model, from which an overall CL_{int} can be calculated. To streamline the data processing, a MATLAB (Mathworks) script was created to fit the mono- and bi-exponential models to the raw data and perform a statistical comparison between them. The two models were compared with the Akaike information criterion (AIC) which was corrected as finite sample sizes were used. The corrected AIC was calculated as follows (Motulsky and Christopoulos 2004):

$$AIC_c = N * \ln\left(\frac{SS}{N}\right) + 2K + \frac{2K(K+1)}{N-K-1}$$

where N is the number of data points, SS is the sum of squares for the model fit and K is the number of parameters fit by the model plus one. In order to determine which model minimised the loss of information, the difference in AIC_C values were calculated:

$$\Delta AIC = AIC_{C,bi-exponential} - AIC_{C,mono-exponential}$$

From this the probability that the bi-exponential model is better than the mono-exponential model was calculated from:

$$Probability(bi-exp.) = \frac{e^{-0.5\Delta}}{1+e^{-0.5\Delta}}$$

The values were then entered into the prediction model to predict *in vivo* clearance.

3.9. Metabolite Identification

The metabolite identification was performed on the Synapt G2 quadrupole time-of-flight (Q-TOF) with electro-spray ionisation (ESI) and Acquity UPLC system (Waters) with the accompanying software Metabolynx (Waters). Ten compounds were chosen to be analysed from the incubation in 1 million cells/ml at three time points (0.5, 45 and 120 min) and were analysed in the positive ionisation mode.

The chromatography was performed on the Acquity UPLC BEH C18 1.7 µm, 2.1x100 mm column at column oven temperature 45°C with a 1 µl injection volume at a carrier flow rate of 0.5 ml/min. A high gradient elution was performed between 0.1% formic acid in water (A) and Acetonitrile (B) in the following profile:

1. 0 min 10 % B
2. 6 min 70 % B
3. 6.01 min 90 % B
4. 6.70 min 90 % B
5. 6.71 min 10 % B

Metabolynx software was used to determine the presence of the predicted metabolites.

4. Results and Discussion

A large amount of data was generated throughout this investigation; therefore only representative data that shows the major findings will be displayed and discussed. It was found that 19 of the 26 test compounds, when metabolised in human liver microsomes, appeared to be stable, which suggests that the dominant clearance route of these compounds was conjugative metabolism rather than additional metabolic routes such as phase I metabolism (oxidation, reduction, de-methylation etc.), this despite the fact that hydroxy metabolites were detected for several of the compounds in the test compound set. In the human liver microsomes, a few of the compounds showed bi-phasic depletion curves, but due to the overall stability, few results could be obtained from these experiments. Therefore all results presented are from experiments with rat hepatocytes.

4.1. Measurement of Viability during Incubation

As a decrease in hepatocyte viability may have an effect on the depletion profile, initial experiments were performed to evaluate the cell viability during the course of the two hour long incubation. A series of viability measurements were performed on the initial cell suspension (3 million cells/ml) after being stored in a water bath for (0, 1 and 2) hours. The viability was also measured of samples that underwent the same two hour procedure on the robot as the metabolic experiments, although no additional chemicals were added to these samples. The results, presented in Figure 5, showed that the viability in the tube did not change more than 5% from the initial value over the two hours of incubation, and for samples that had been incubated on the robot, as in the assay, there was a decrease in viability by less than 10%. This small decrease in viability would not likely affect the overall enzyme activity enough to have an impact on the shape of the depletion curve and neither would the organic solvents in the incubation mixtures. The incubation mixtures contained 1% ACN and 0.01% DMSO, and while DMSO has been shown to have inhibitory effects, the concentration used in this study may be low enough to not affect the enzymatic activity (Easterbrook, Lu et al. 2001). Previous studies have concluded that ACN does not have any significant effects up to concentrations of 1% and that it is the most suitable organic solvent for these investigations (Easterbrook, Lu et al. 2001, Li, Han et al. 2010). During drug development, the intrinsic clearance is determined before the compounds are tested for toxicity, and therefore toxic compounds might decrease the viability during the incubation. However, it is very unlikely

that this can explain the bi-phasic depletion behaviour as established drugs on the market, including Diclofenac and Telmisartan, also showed this bi-phasic depletion profile. Based on these viability measurements, it is unlikely that a decrease in viability during incubation has a major impact on the experimental metabolic stability data and the shape of the depletion curve.

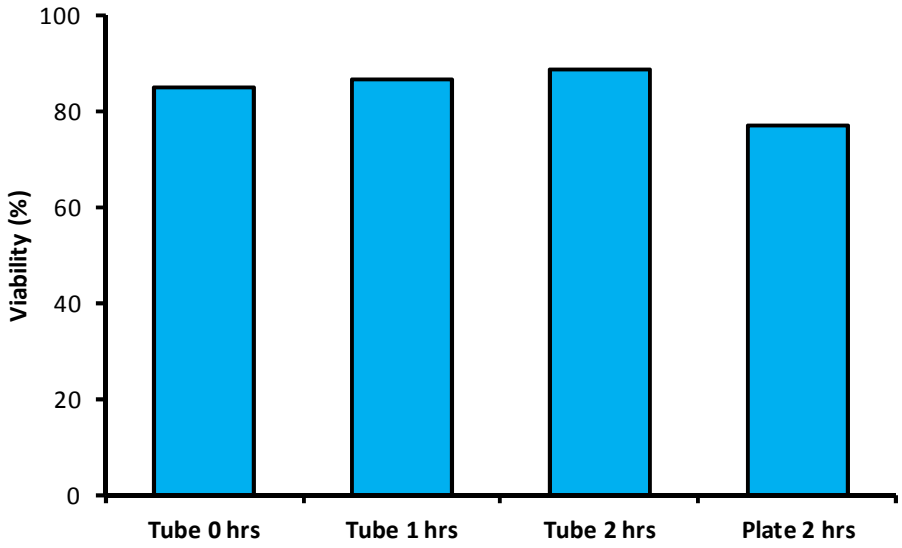

Figure 5. Viability of rat hepatocytes incubated at 37ºC in a tube after (0, 1 and 2) hours and after 2 hours of shaking in plate at 37º C on the robot. These experiments showed that the viability of the cells did not significantly change over the two hour incubation.

4.2. Chromatographic and Mass Interferences

Another factor that could have an impact on the shape of the depletion curve is interferences from the analytical setup. To investigate the occurrence of chromatographic and mass interferences, as described in section 1.4, the results from the chromatography performed on the three different columns were compared. The three different columns were all of the same length but had different separation characteristics. As shown in Figure 6a, the choice of column did not affect the calculated CL_{int} values for AZ_01. The formation of the acyl glucuronide, shown in Figure 6b, appeared to occur the first 30 min of incubation before slowly decreasing over the remainder of the experiment. This time point was cohesive with the shift in gradient in the depletion of the test compound, however there was no co-elution of the compounds so the breakdown of the acyl glucuronide back to test compound in the mass spectrometer was not likely to contribute to the response signal and shape of the depletion

curve. The values of CL_{int} calculated from the results in Figure 6 are listed in Table 1 and show that the choice of column did not have an impact the final CL_{int} value for this compound.

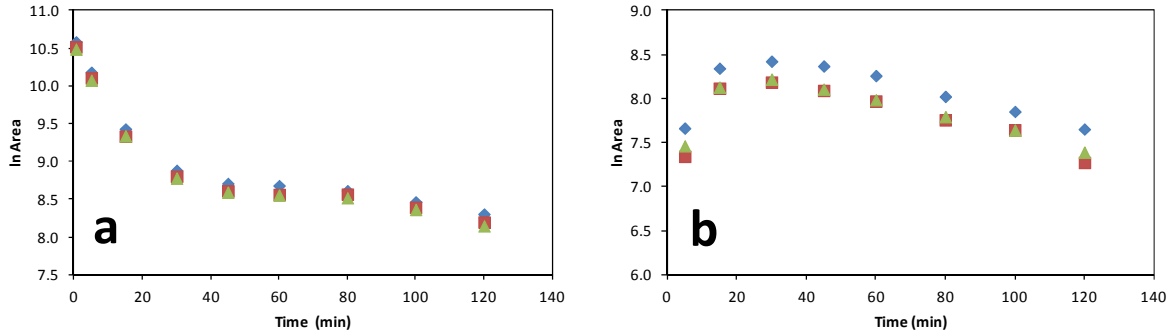

Figure 6. a) Depletion and b) acyl glucuronide formation of compound AZ_01 at a cell concentration of 1 million cells/ml measured from chromatographic separation on the HSS T3 (diamonds), CSH (squares) and BEH C18 (triangles) columns on short gradient elution.

Table 1. Calculated CL_{int} values for compound AZ_01 at 1 million cells/ml after chromatographic separation with the HSS T3, CSH and BEH C18 columns on a short gradient elution. The first value was calculated from all data points, while the first phase was calculated from the first two data points.

Column	**CL_{int} (µl/min/10^6)**	
	All Phases	First Phase
HSS T3	16.1	89.2
CSH	16.2	90.8
BEH C18	16.4	91.5

Not all compounds showed the same consistency between each of the three columns; however they did follow the same overall shape of the curve. The separation of the glucuronide and AZ_10 compound on the three chromatographic columns is shown in Figure **7**, where the main shaded peak corresponds to the AZ_10 compound and the smaller initial peak is the acyl glucuronide. The two compounds were shown to be adequately separated with the HSS T3 and CSH columns, although the former showed a greater separation. However, the BEH column was unable to effectively separate the compounds and hence the test compound and the acyl glucuronide were co-eluted. As an acyl glucuronide fragments into the test compound in the ion source, (as described in section 1.4) and behaves like the

test compound, it will very likely contribute to the peak area of the test compound when co-eluted, which would change the gradient of the depletion curve.

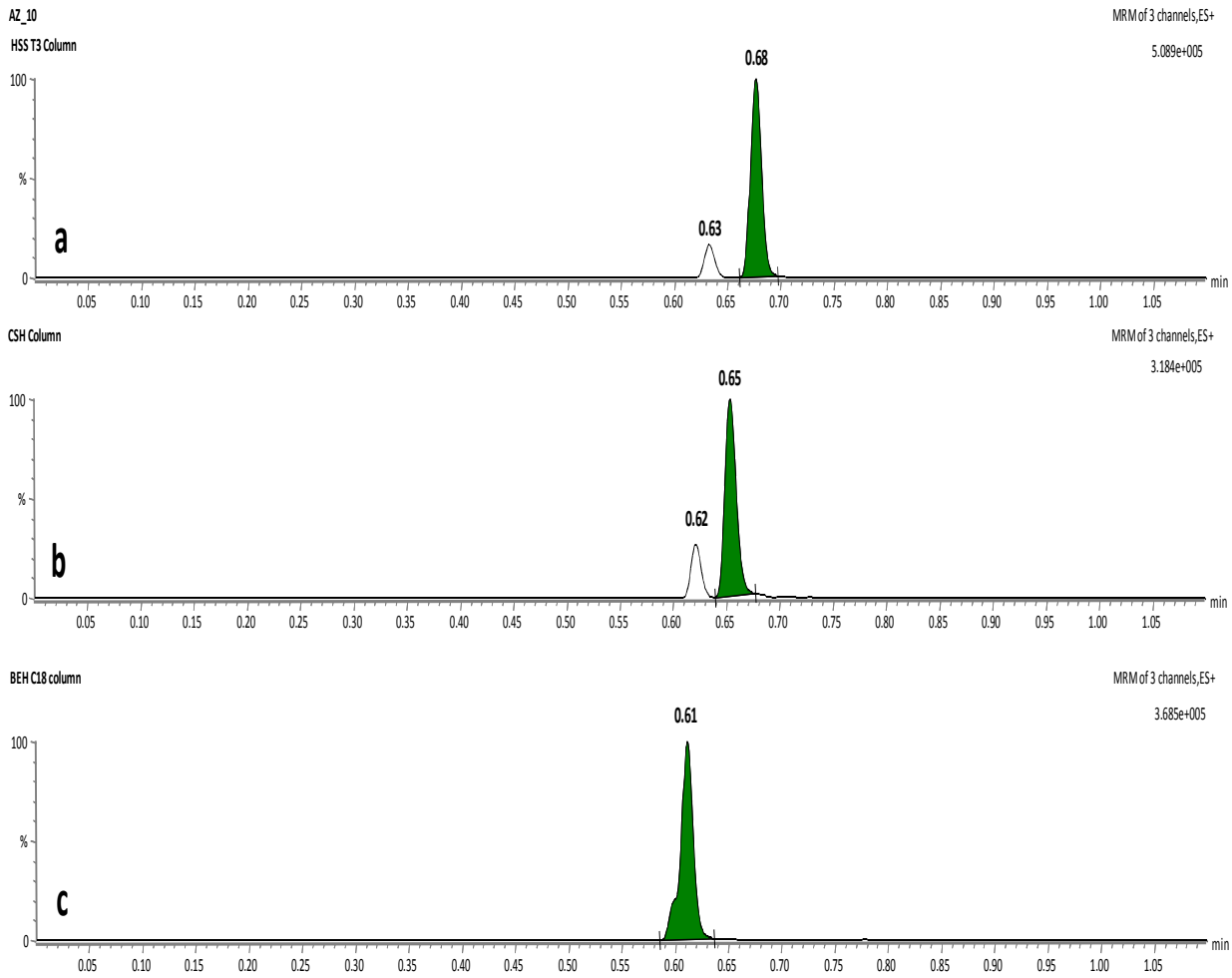

Figure 7. Chromatograms for AZ_10 after separation on the a) HSS T3, b) CSH and c) BEH C18 columns with a short gradient elution and analysis with Triple Quadrupole (TQD) LC-MSMS. Note that the two peaks were separated on the HSS T3 and CSH columns whereas the peaks were co-eluted on the BEH C18 column.

The depletion curves of AZ_10 obtained with the HSS T3 and CSH columns had a near identical trend (Figure 8), although they were vertically offset from each other, which suggest that there was a variation in response caused by compound instability during the analysis. The analysis of the samples for all three columns took approximately 72 hours to complete and the stability of the compounds during this time could only be assumed to be constant. Breakdown of the compound over time could possibly explain the observed vertical offset. Furthermore, formation of the acyl glucuronide occurred in the first 30 minutes, similar to

compound AZ_01 (Figure 6), although the depletion curve did not exhibit a bi-phasic profile. As the BEH C18 column was unable to separate the acyl glucuronide from AZ_10, no separate acyl glucuronide values were obtained for this column and the depletion curve showed a different trend to the other two columns.

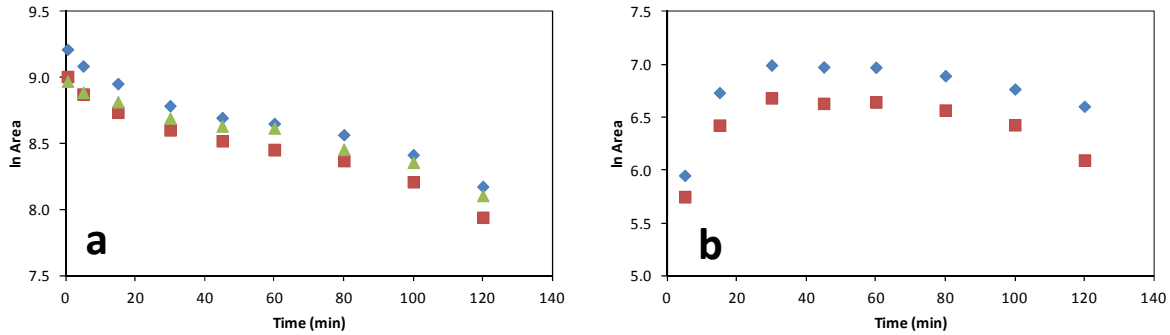

Figure 8. a) Depletion curves of AZ_10 and b) formation curve of the glucuronide at 1 million cells/ml after separation on the HSS T3 (diamonds), CSH (squares) and BEH C18 (triangles) columns. Note that the glucuronide was not separated from AZ_10 in the BEH C18 column so no values were obtained for it.

The impact of chromatographic separation on different columns on the calculated CL_{int} values for compound AZ_10 were evaluated and are displayed in Table 2. When including all data points, there was no difference in calculated CL_{int}, between the HSS T3 and the CSH columns. The CL_{int} value generated from the BEH C18 column data were slightly lower, which could be explained by the contribution of the co-eluted acyl glucuronide. The CL_{int} values obtained from the first phase the data from HSS T3 and CSH columns were again similar, and in this case the value obtained from the BEH C18 column data was a third lower, which clearly shows that the inadequate separation on this column had an impact on the calculated CL_{int} value.

Table 2. Calculated CL_{int} for AZ_10 at 1 million cells/ml after separation with the HSS T3, CSH and BEH C18 columns. The first value (all phases) was calculated from all data points, whereas the first phase was calculated from the first two data points.

Columns	**CL_{int} (µl/min/10^6)**	
	All Phases	First Phase
HSS T3	7.5	28.1
CSH	7.6	29.7
BEH C18	6.3	18.9

Overall, the best chromatographic separation between the test compounds and measured metabolites for all tested compounds was achieved on the HSS T3 and CSH columns; however this had no impact on the calculated CL_{int} values. The chromatographic separation with the BEH C18 column was adequate, with one exception where co-elution was observed which was reflected in the calculated CL_{int} values. When calculating the CL_{int} value based on only the first phase small variations in the measurements can have a major impact on the results as the number of data points to include in the first phase are few and the selection is subjective. In many cases, only two data points are included which makes the values uncertain. The deviation in CL_{int} value could be due to small variations in measurements, but the co-elution of the acyl glucuronide is likely an important factor, however this does not contribute to the bi-phasic profile. Although the columns performed very similar, most of the following results were produced using data from the HSS T3 column as this column is the standard one for this assay.

4.3. Impact of Protein Concentration on the Depletion Curve

To assess the importance of protein concentration for the shape of the depletion curve the experiments with hepatocytes were performed using three different cell concentrations; 0.25, 1 and 2 million cells/ml. For all compounds the calculated CL_{int} values decreased with higher cell concentration, after normalising values to the cell concentration with three examples visualised in Figure 9. For some compounds, like Atorvastatin, the difference in intrinsic clearance was large between the cell concentrations, whereas the protein concentration had only a minor effect on intrinsic clearance for other compounds including AZ_03. Most of the compounds, such as AZ_01 fell in between these two extremes. These results suggest that the metabolic turnover is higher as the cell concentration decreases which may be explained by a larger fraction of unbound compound being available for metabolism.

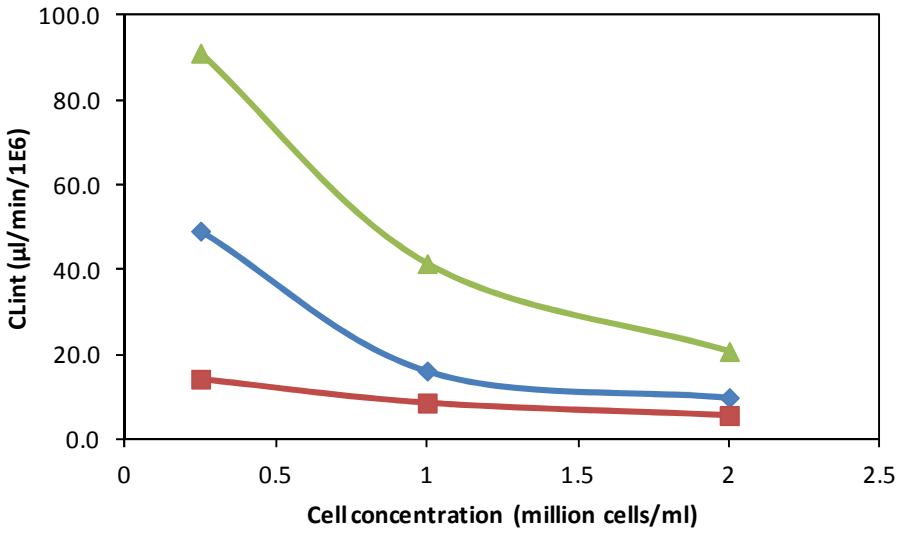

Figure 9. Calculated CL_{int} values at different cell concentrations for AZ_01 (diamonds), AZ_03 (squares) and Atorvastatin (triangles). The chromatography was performed on a HSS T3 column.

Depletion curves for all compounds at all three concentrations were plotted on a logarithmic scale for each experiment. The controls showed a linear profile for all cell concentrations, while the depletion profile of the commercial and AZ compounds varied from bi-phasic to linear to stable. In the set of 26 test compounds, 10 of them changed shape of the depletion curve towards more linear or stable at lower cell concentrations, 11 were biphasic at all cell concentrations, 2 were stable and 3 had a linear depletion curve.

A comparison was made between the compounds that had a bi-phasic depletion curve for all three cell concentrations and the compounds where the depletion curve changed in shape for the three cell concentrations. The LogD values for this set of compounds ranged between -0.1 and 2.8. It was found that among the compounds that had a bi-phasic depletion curve for all three cell concentrations, e.g. AZ_08 (Figure 10a), most of them had a low LogD value. For compounds where the depletion curve appeared to become more linear or stable as the cell concentration decreased, e.g. AZ_05 (Figure 10b), the LogD values were predominantly higher than the compounds with a bi-phasic depletion curve at all three cell concentrations.

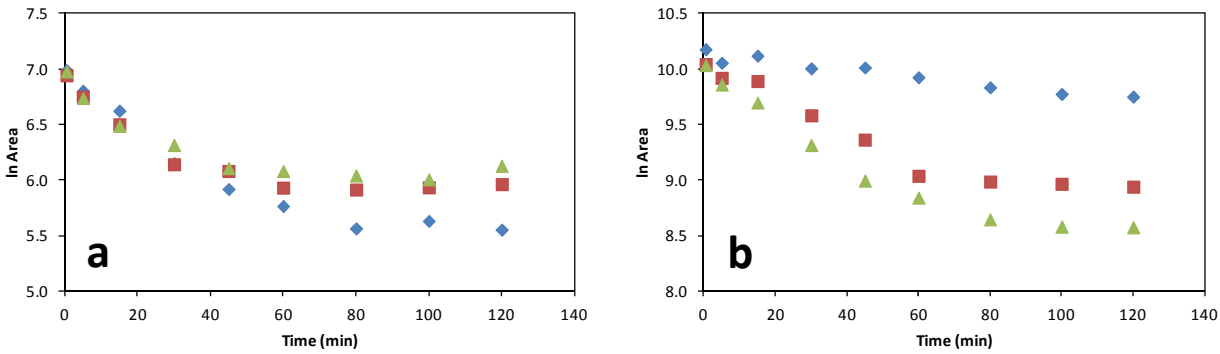

Figure 10. Depletion curves of a) AZ_08 (LogD=0.2) and b) AZ_05 (LogD=1.7) at cell concentrations 0.25 million cells/ml (diamonds), 1 million cells/ml (squares) and 2 million cells/ml (triangles).

A comparison between the compounds that had a bi-phasic depletion curve for all three cell concentrations and those that the depletion curve changed shape, showed a statistically significant difference between the LogD values (Figure 11). Although there were some outliers, the trend was clear and cohesive with Figure 10.

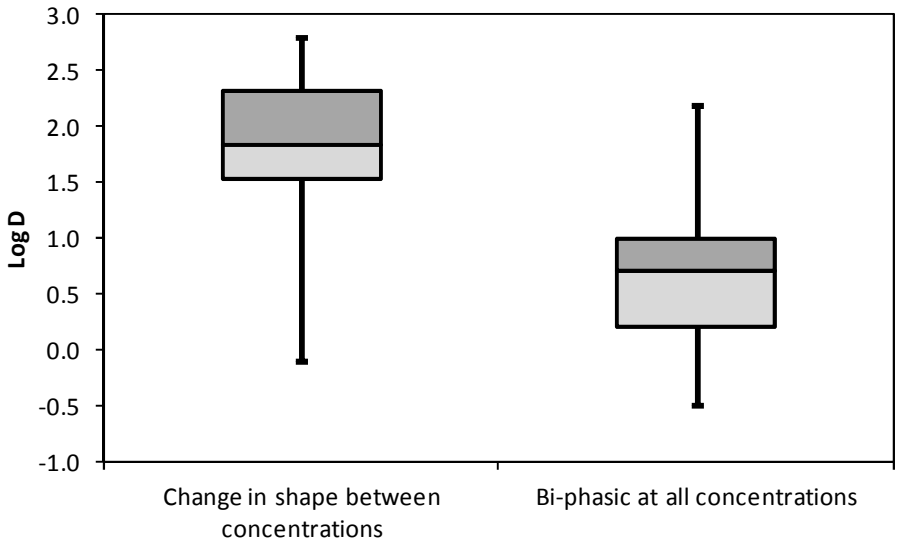

Figure 11. A box and whisker plot of LogD values of compounds with different shaped depletion curves at different cell concentrations (n=10), and LogD values of compounds with bi-phasic depletion curve for all measured cell concentrations (n=11).

Another thing worth noting is that for AZ_08 (Figure 10a) the depletion during the first 15-30 minutes appeared to be independent of cell concentration with about 60% and 40% remaining

at 15 and 30 min respectively. The concentration of the compound was then stabilised at a remainder of about (40, 35 and 20) % for (2, 1 and 0.25) million cells/ml respectively. The reason for this can only be speculated, a possible explanation could be metabolite inhibition of the enzyme or a multiple enzymes involved, or multiple sites of metabolism.

4.4. Confirmation of Metabolite Identity

Metabolites formed during incubation may contribute to the response signal and hence also the shape of the depletion curve. To test this, the most likely metabolites were detected by multiple reactions monitoring of the transitions determined in optimization process by using QuanOptimize (Waters). The acyl glucuronides were expected in the same transitions as the test compounds if the chromatographic separation was achieved. The hydroxy metabolites were detected using semi single reaction monitoring data acquisition, allowing comparison of depletion of the test compound and the formation of the metabolite. Acyl glucuronides were detected for 15 of 19 bi-phasic compounds and for 2 of the 7 linear compounds along with 4 and 2 hydroxy metabolites detected for bi-phasic and linear compounds respectively. From this small set of compounds no conclusions can be drawn, but it appears as if acyl glucuronides are present to a larger extent in compounds with bi-phasic depletion behaviour and the hydroxy metabolites are present in both. The hydroxy metabolite was detected for AZ_12 and the depletion of the test compound and the formation of hydroxy metabolite are shown in Figure 12. It was observed that as the test compound at a cell concentration of 2 and 1 million cells/ml was metabolised the metabolite was formed. At the 0.25 million cells/ml cell concentration, the compound appeared to be stable but the metabolite was still formed.

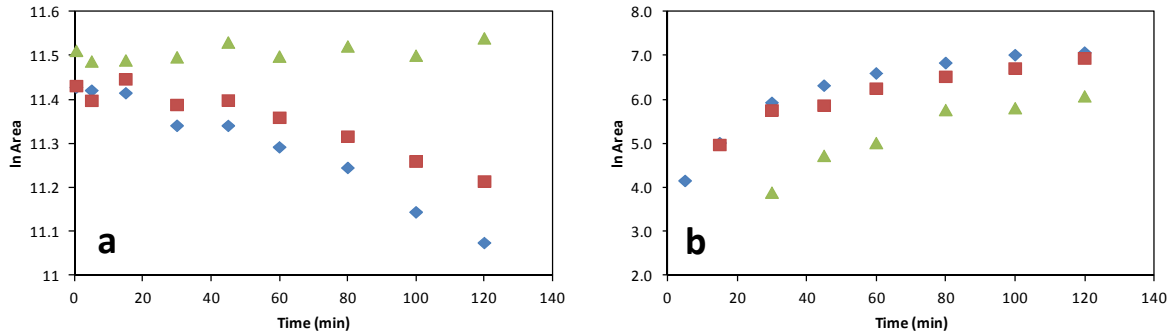

Figure 12. Depletion curve for a) AZ_12 and b) formation of hydroxy metabolite at cell concentrations 0.25 million cells/ml (triangles), 1 million cells/ml (squares) and 2 million cells/ml (diamonds).

The CL_{int} values were calculated for the depletion of the compound as well as for the formation of hydroxy metabolite and are listed in Table 3. The rates of depletion of the test compound and the formation of the metabolite were similar for the cell concentrations 1 and 2 million cells/ml, but at 0.25 million cells/ml the compound appeared stable with a calculated CL_{int} lower than 1. However, there was a rapid formation of the metabolite (89.2 µl/min/10^6 for all data points and 222.8 µl/min/10^6 for the first phase) and it is not unlikely that this rapid formation contributes to the shape of the depletion profile even if the mass response of the hydroxy metabolite cannot be used to calculate concentrations and therefore the difference in absolute concentration cannot be determined.

Table 3. Intrinsic clearance of AZ_12 and the formation of hydroxy metabolite calculated for all data points and the first phase.

	Bi-phasic formation of metabolite		Linear depletion
	µl/min/10^6		CL_{int} (µl/min/10^6)
Cell concentration (million cells/ml)	All Points	First Phase	
2	11.5	42.9 (2 points)	1.5
1	17.0	52.1 (2 points)	1.8
0.25	89.2	222.8 (2 points)	< 1

To investigate the possible contribution to the curve profile by the metabolite, the chromatograms were inspected (Figure 13). Multiple possible hydroxy metabolites were detected (Figure 13a), and it was found that for AZ_12 the test compound and one of the hydroxy metabolites co-eluted on all three columns when analysed on the short gradient. In addition, the acyl glucuronide was detected on the same trace as the test compound (Figure 13b).

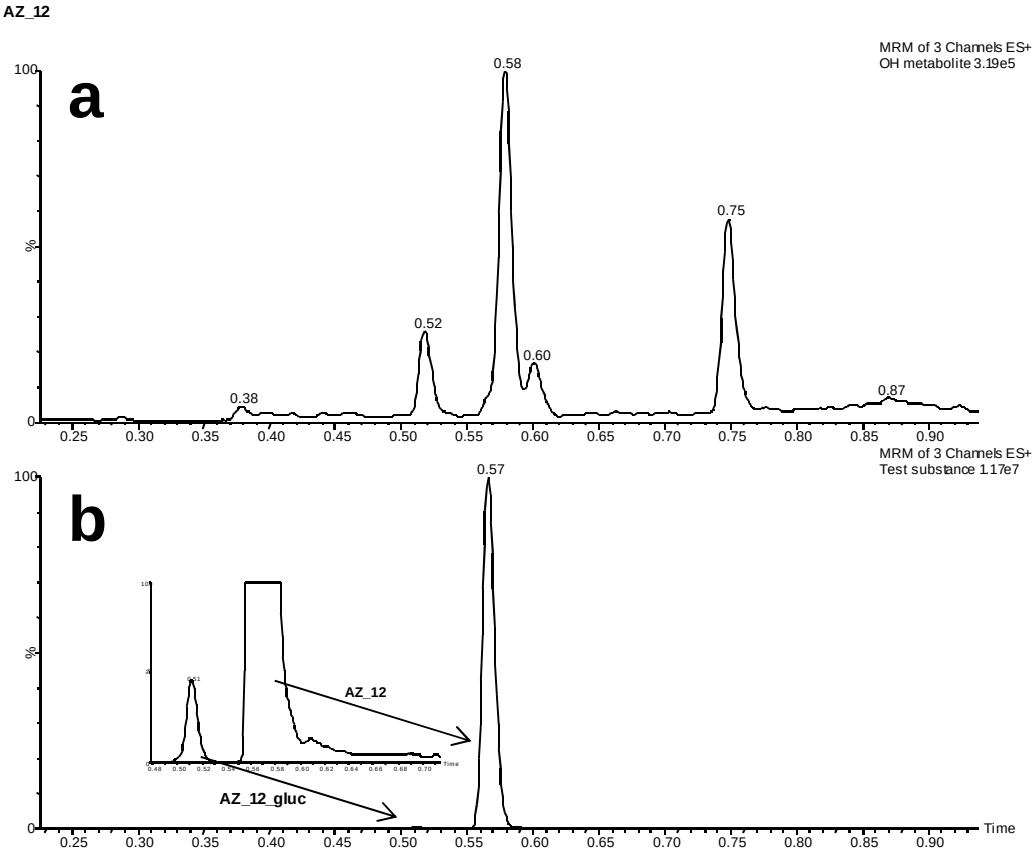

Figure 13. Chromatogram for AZ_12 from analysis on short gradient elution on HSS T3 column with a) hydroxy metabolite and b) the test compound and the thermally labile acyl glucuronide. Co-elution of test compound and hydroxy metabolite occurred.

To confirm the identity of the metabolites, the samples were also analysed on a long gradient chromatography and Q-TOF. The long gradient provided better separation between compounds, although the co-eluting peaks on the short gradient were still slightly overlapped. The spectrums for the test compound and the acyl glucuronide were inspected and their identities were confirmed and multiple hydroxy metabolites were detected (Figure 14).

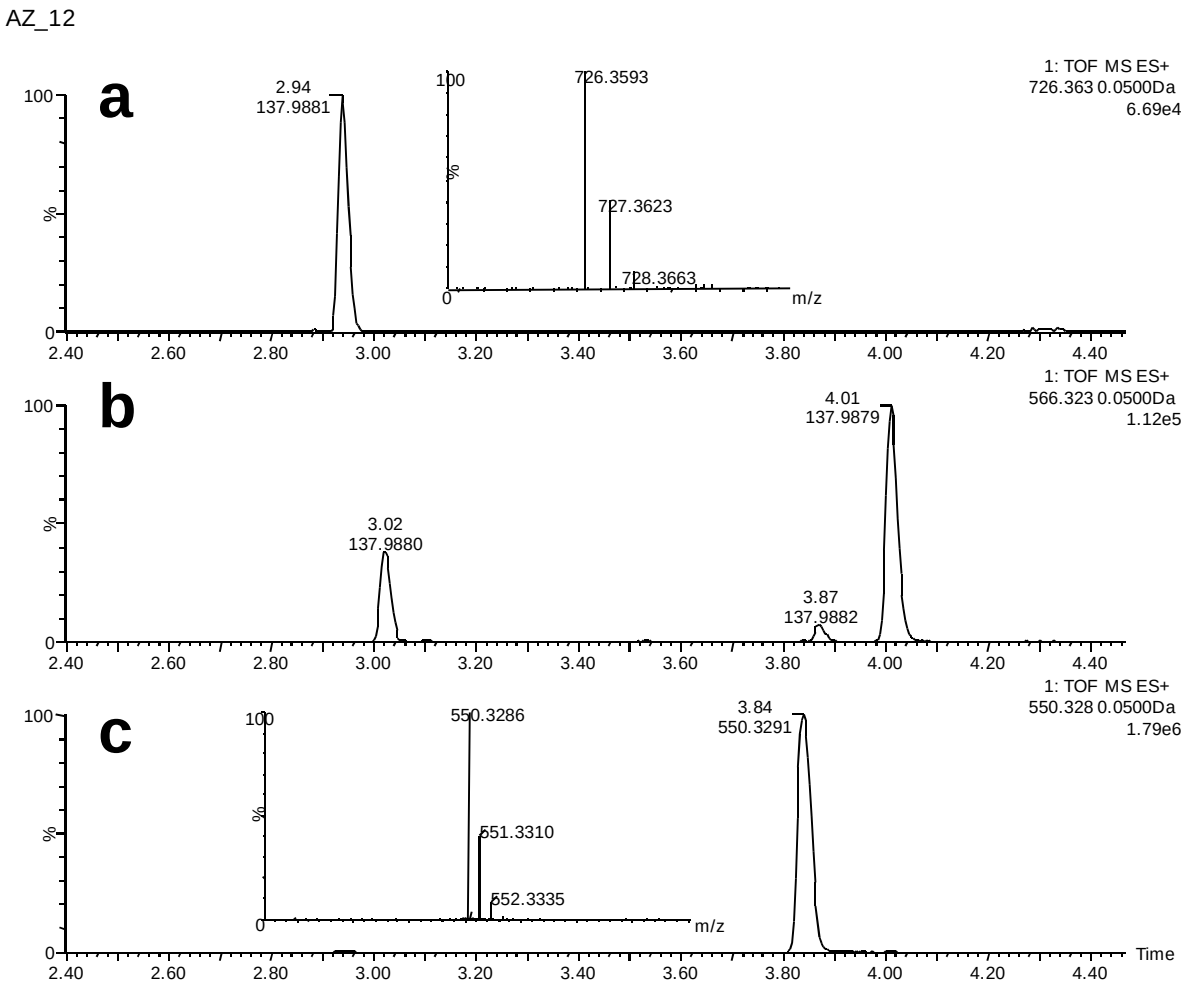

Figure 14. Chromatogram for AZ_12 from separation on BEH column using a long gradient and analysis on Q-TOF. Detected compounds were the a) acyl glucuronide, b) hydroxy metabolites and c) the test compound. The identities of the test compound and acyl glucuronide were confirmed by TOF data.

The spectrums for the three peaks shown in Figure 14b were studied to identify the possible hydroxy metabolites (Figure 15). The peaks eluted at 3.02 min and 4.01 min could be confirmed to be hydroxy metabolites from the top and bottom traces. The smaller peak eluted in between the two peaks had a spectrum identical to the spectrum of the test compound suggesting that this metabolite fragments into the test compound in the ion source. If the three large peaks from the long gradient chromatography corresponded to the same metabolites as the three largest peaks on the short gradient chromatography, then the metabolite that co-eluted with the test compound was the one that breaks into the test compound. It is very likely that this metabolite contributed to measured peak area and may explain why the compound appeared to be stable at 0.25 million cells/ml. Although,

compound AZ_12 was the only compound with a co-elution of the hydroxy metabolite and the test compound and despite that, it had a linear depletion curve. Because of that it can be concluded that this co-elution does not cause bi-phasic depletion behaviour.

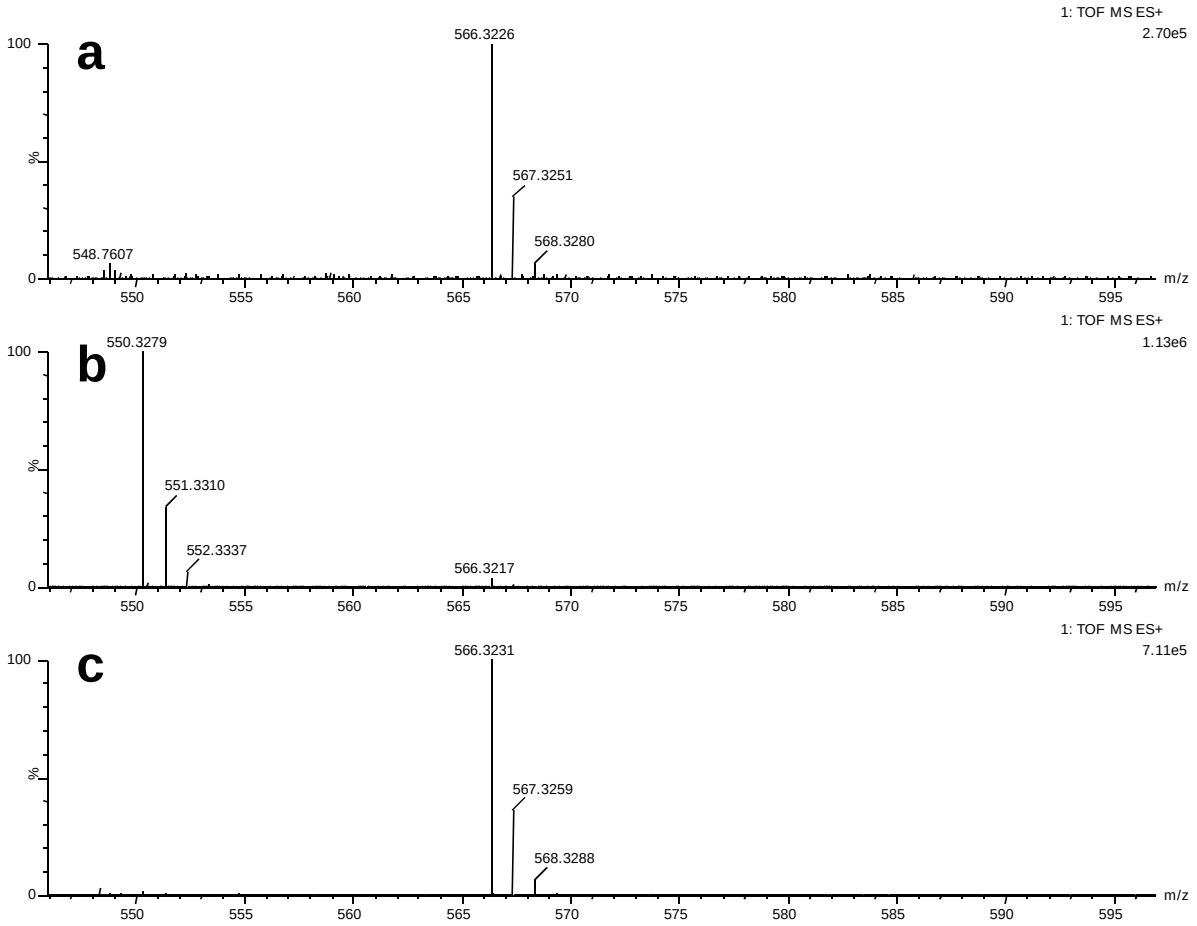

Figure 15. Spectrums of the tree peaks caught on the hydroxy metabolite trace in Figure 14. a) and c) could be confirmed to be hydroxy metabolites. The compound in b) was most likely a hydroxy metabolite that fragmented into the test compound in the ion source.

4.5. Data Modelling for Objective Calculations of CL_{int}

The bi-phasic depletion was modelled as a means to objectively calculate the CL_{int} with a reduced risk of underestimation. The data was normalised to 100 % and fit to a mono-exponential model (red line) and a bi-exponential model (blue line). The results for AZ_12 and AZ_01 at 1 million cells/ml are visualised in Figure 16 and the fitting parameters with confidence intervals and the goodness-of-fit values can be seen in Table 4. The two models overlap for AZ_12 (Figure 16a) which is a strong indicator that the depletion is linear on a

logarithmic scale. Furthermore, the confidence intervals for the parameters are large for the bi-exponential model, suggesting it is a poor model for this set of data. By visual inspection of Figure 16b the bi-exponential model fits the data set very well, and even though R^2 adjusted is not an absolute indication of the fit, the value of this model for AZ_01 is 0.999 which is near enough perfect fit to the data points.

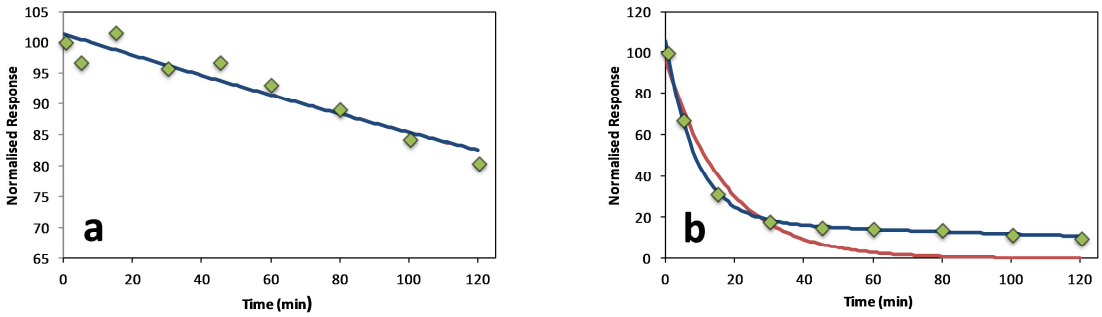

Figure 16. Mono-exponential model (red line) and Bi-exponential model (blue line) fit to normalised response at all time points at 1 million cells/ml for a) AZ_12 and b) AZ_01. For AZ_12 the two models overlap which means that the depletion is mono-exponential. For AZ_01 the two models are fit to the data differently.

Table 4. Fitting parameters with confidence intervals and goodness-of-fit for a mono-exponential model and a bi-exponential model for AZ_12 and AZ_01 at a cell concentration of 1 million cells/ml.

AZ_12						
	Coefficients	**Values**	**CI 2.5%**	**CI 97.5%**	**Goodness-of-fit**	**Value**
Mono-exp.	a	101.30	98.12	104.47	**sse**	4.096E+01
	b	-0.002	-0.002	-0.001	**R^2**	8.992E-01
					df	7.000E+00
					R^2 adj.	8.849E-01
Bi-exp.	a	0.00	-36.6E+06	36.6E+06	**sse**	4.096E+01
	b	0.00	-36.7E+06	36.7E+06	**R^2**	8.992E-01
	c	101.29	-36.6E+06	36.6E+06	**df**	5.000E+00
	d	0.00	-50.40	50.40	**R^2 adj.**	8.388E-01
AZ_01						
	Coefficients	**Values**	**CI 2.5%**	**CI 97.5%**	**Goodness-of-fit**	**Value**
Mono-exp.	a	96.41	73.69	119.13	**sse**	7.679E+02
	b	-0.06	-0.09	-0.03	**R^2**	9.015E-01
					df	7.000E+00
					R^2 adj.	8.875E-01
Bi-exp.	a	87.02	83.66	90.38	**sse**	2.831E+00
	b	-0.12	-0.13	-0.11	**R^2**	9.996E-01
	c	18.25	15.16	21.34	**df**	5.000E+00
	d	-0.004	-0.006	-0.002	**R^2 adj.**	9.994E-01

To compare the models, the Akaike Information Criterion scores were calculated for both models and from that the probability that the bi-exponential model is the best for this data set was calculated (Table 5). For AZ_12 this probability was 0 and for AZ_01 the probability was 1, which agrees with the visual presentation for the depletion of both compounds (Figure 16). The CL_{int} values for the two models were also calculated and along with the corrected values based on the bi-exponential model (Table 5). For AZ_12 the corrected value corresponded perfectly to the value calculated from the mono-exponential model suggesting that the bi-exponential model, when corrected, produced representative data. For AZ_01 the corrected value was closer to the uncorrected value from the bi-exponential model (2 exp alpha), which could be expected from the high probability of the bi-exponential model and the visual inspection of the depletion curve. A bi-exponential decay model approach has previously been used by Jigorel and Houston for the calculated CL_{int} values, but they used no correction term and assumed the first depletion constant to be representative as the decay constant for the first phase (Jigorel and Houston 2012).

Table 5. Akaike Information Criterion scores and calculated CL_{int} values for mono-exponential model and bi-exponential model for AZ_12 and AZ_01at 1 million cells/ml.

AIC	**AZ_12**	**AZ_01**
AIC_c mono-exp	24.44	50.82
AIC_c bi-exp	43.64	19.59
ΔAIC (bi-mono)	19.20	-31.23
Probability (bi-exp)	0.00	1.00
CL_{int} (µl/min/million cells)		
1 exp (all)	1.71	58.03
1 exp (alpha)	1.71	89.20
2 exp (alpha)	2.00	117.30
2 exp (beta)	1.71	4.18
Bi-exp. corrected	1.71	97.68

For most compounds this method to choose the right model for the depletion of the compound and the calculation of CL_{int} was adequate and objective, however there are some limitations. The model needs a minimum of 4 data points to make the bi-exponential fit and

the Akaike Information Criterion scores need more than 7 data points to be able to make the calculations to compare these two models. The assay set up collects a maximum of 9 data points which can be a problem for rapidly metabolised compounds that generate fewer data points. These two compounds that are presented as examples are two very clear examples of linear and bi-phasic depletion and that is why the probability was calculated to 0 and 1. Some of the other compounds fall in between but maybe the model does not have to be chosen, with the bi-exponential model and the correction term the calculated CL_{int} value will still correspond to the mono-exponential value if the depletion is linear. The current way of producing the CL_{int} values from compounds in high throughput screening works for the majority of the compounds but becomes a problem when faced with a bi-phasic depletion curve. To eliminate the human factor of the determination of the CL_{int}, an objective calculation model is highly needed and as such this approach could be useful.

4.6. Impact of Choice of Model on the Predictions of in vivo Clearance

The CL_{int} values calculated for the mono-exponential model (using all data points and the first phase respectively) were entered into the prediction model and produced two different values for the *in vivo* clearance. The values are compared in Figure 17. Many of the compounds are found near the dashed line indicating that the prediction for these compounds is not likely to be affected by which of the two CL_{int} values the calculation is based on. The hepatic blood flow of a rat (and therefore the maximum blood clearance rate) is 72 ml/min/kg (Sohlenius-Sternbeck, Jones et al. 2012) and this value was used to calculate the fraction of the maximum blood clearance for each prediction. Three compounds (circled in the figure) had a fraction difference of more than 30 %, and in these cases the choice of CL_{int} value does have an impact on the prediction. Six other compounds had a fraction difference of 10-20% between the two calculation models. When the blood clearance values were converted to plasma clearance (conversion factor 0.55 for acids (Sohlenius-Sternbeck, Jones et al. 2012)) the prediction for the first phase was closer than the prediction derived from all data points to experimental data of *in vivo* plasma clearance; however the amount of *in vivo* data was very limited and only available for 3 of the test compounds, and no conclusions could be drawn from that small comparison (For the plasma clearance predictions data see Appendix I). Despite that, it does seem likely that the predictions will be in better agreement with in *vivo data* when they are based on the higher CL_{int} values derived from the first phase. When the predictions generated from the mono-exponential model for the first phase and the corrected

values generated from the bi-exponential model were compared they did not deviate at all (Figure 18). This suggests that the prediction was independent of which of the models was used, however, as the mono-exponential model for the first phase is subjective and the bi-exponential model is objective and includes all points, and again, an objective method including all data points is more robust and reproducible.

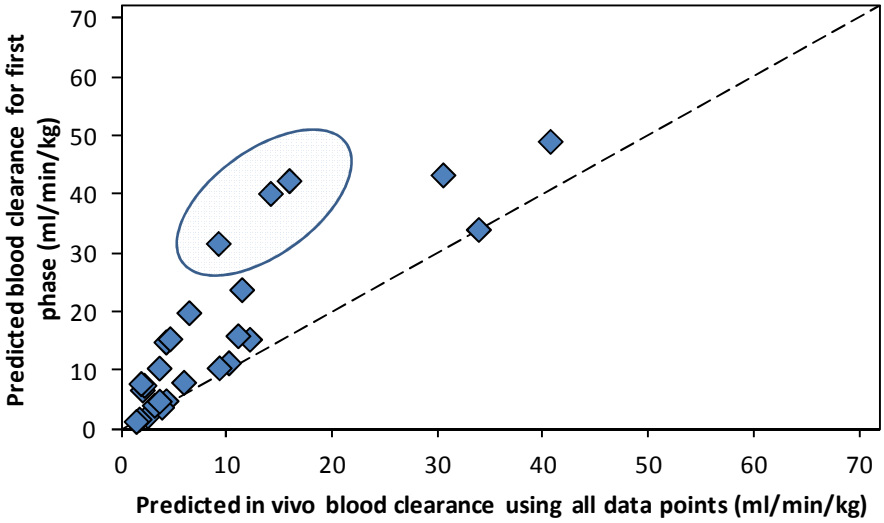

Figure 17. Comparison of predictions of *in vivo* blood clearance using a mono-exponential model with values calculated from the first data points and all data points for all test compounds at a 1 million cells/ml concentration. The compounds where the difference between the fractions of maximum blood clearance of the predictions was more than 30% are circled.

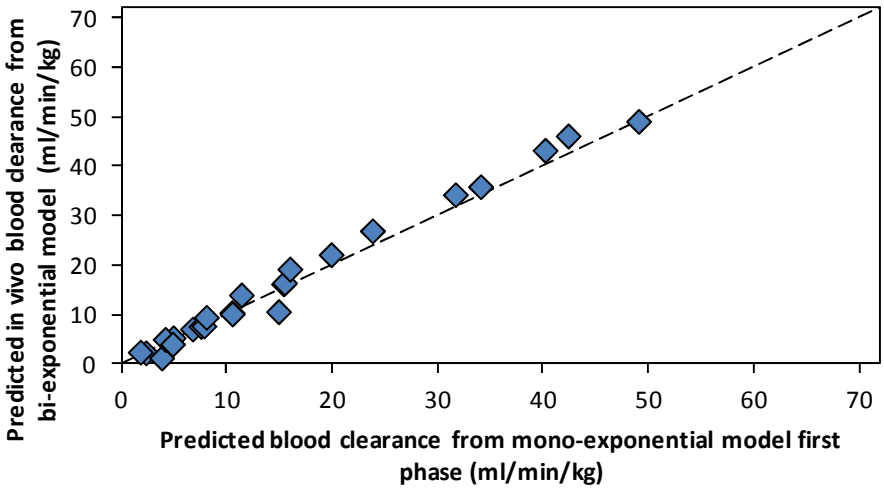

Figure 18. Comparison of predictions of *in vivo* blood clearance between the first phase with a mono-exponential model and a bi-exponential model for all test compounds at a 1 million cells/ml concentration.

4.7. Assessment of the Importance of True Zero

To investigate the importance of the true initial compound concentration for the depletion curve (in the standard assay the first time point is 0.5 min) an experiment where the cells were lysed before the addition of compound was performed. The difference in peak area between the true zero sample and the first time point 0.5 min ranged between 1% and 40% with an average of about 20%. Two compounds with the average difference between the 0 point and the 0.5 time point were Atorvastatin with a linear depletion curve and AZ_11 with a bi-phasic depletion curve. The disappearance of the compounds between the first two time points can be seen in Table 6.

Table 6. Disappearance of Atorvastatin and AZ_11 during the first two time intervals of incubation.

Disappearance	Atorvastatin	AZ_11
Between 0 and 0.5	- 20 %	- 21 %
Between 0.5 and 5	- 25 %	- 34 %

The depletion curves of the two compounds were modelled with a mono-exponential model for Atorvastatin (Figure 19a) and a bi-exponential model for AZ_11 (Figure 19b) including the zero points (squares in the figures) and can be seen as the curves in the figures.

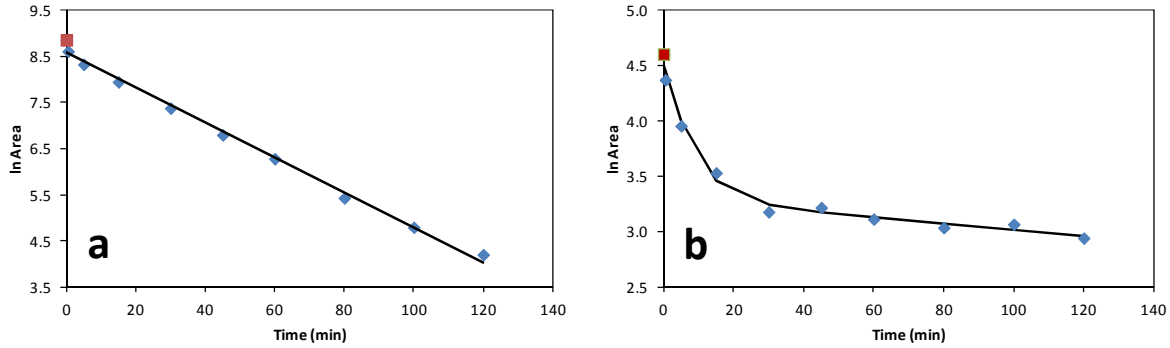

Figure 19. Depletion curves of a) Atorvastatin and b) AZ_11 with true zero as squares in the figure. A mono-exponential model to all data points (including zero) has been fit to Atorvastatin and a bi-exponential model has been fit to all data points (including zero) for compound AZ_11. The models are visualised as curves in the figures.

From the models, CL_{int} values were calculated by including or excluding the zero time point (Table 7). For AZ_11 the calculations were performed using both models. For linear compounds like Atorvastatin, there was no difference between the values including the zero time points, which could be expected if the depletion curve is linear. For the bi-phasic compound AZ_11 the CL_{int} values calculated on the first two points, including or excluding the zero time point, agreed very well with the values produced by the bi-exponential model. The CL_{int} value for AZ_11 changed about 20 % when the zero point was included which is not likely to have a major impact, but could potentially cause a slight under prediction. From the setup for the assay of this project it is not possible to distinguish between uptake and metabolism rate limitations as the cells are lysed when the reactions are stopped. It has previously been shown that some compounds metabolise at the same rate as the disappearance of the compound from the medium, strongly suggesting that they are uptake rate limited, whereas other compounds, such as Atorvastatin, have a bi-phasic disappearance from the cell medium but a linear depletion (Jigorel and Houston 2012). There is a possibility that the bi-phasic depletion profile can be observed for compounds where the metabolism is uptake rate limited.

Table 7. Calculated Clint values of compound AZ_11 using a mono exponential model at different number of points and a bi exponential model including all data points including and excluding the zero point. The values calculated from the bi-exponential model have been corrected.

Atorvastatin		AZ_11			
Mono-exponential model		Mono-exponential model		Bi-exponential model	
No. of data points	CL_{int}	No. of data points	CL_{int}	No. of data points	CL_{int}
All	37	2	92	All	92
All + zero point	38	3	55	All + zero point	114
		4	38		
		All	9		
		1 + zero point	465		
		2 + zero point	115		
		3 + zero point	65		
		4 + zero point	44		
		All + zero point	11		

Rapidly metabolized compounds and compounds with a low response on the mass spectrometer were also investigated for the importance of the true zero value. Just as for Atorvastatin, the CL_{int} values were found to match each other very well. This shows that the metabolic rate was not significantly affected by solubility issues for this set of compounds.

5. Conclusions

In this study, a number of parameters that could influence the compound depletion profile were investigated. Also models for calculating CL_{int} values were developed and compared. The metabolic incubations in liver microsomes resulted in 19 of 26 test compounds appearing stable, which suggests that the conjugative metabolism dominated for most of the compounds in this test set. The change in viability of the hepatocytes was negligible during the course of the metabolic incubation and is not likely to contribute to the bi-phasic depletion profile.

The hypothesis that there may be a contribution to the response signal for the test compound from mass or chromatographic interferences could not be confirmed; the short gradient provided adequate separation for most compounds in the test set. Although, for one of the compounds a co-eluted hydroxy metabolite was observed and for one compound the acyl glucuronide co-eluted. Co-elution likely contributes to the shape of the curve and consequently also on the CL_{int} value, but still cannot explain the bi-phasic nature of the depletion curves.

The CL_{int} values decreased as the cell concentration increased. For most compounds of this test set, there was a correlation between the change in shape of the depletion curves and the LogD values. Compounds with low LogD were more prone to be bi-phasic at all the three cell concentrations of this study whereas there was a general change from bi-phasic towards more linear or stable as the cell concentration decreases for compounds with high LogD. Unspecific binding to the phospholipids or proteins of the cell membranes may explain the change in the shape of the depletion and could be a contributing factor to the bi-phasic nature.

The identities of the predicted hydroxy and acyl glucuronide metabolites detected on the triple quadrupole mass spectrometer with short gradient elution using single reaction monitoring were confirmed on the Q-TOF. Acyl glucuronides were detected for 15 of 19 compounds with a bi-phasic depletion curve and for only 2 of the 7 compounds with linear depletion curve. The acyl glucuronides were not co-eluted with the test compounds, with one exception, and so cannot be the cause of the bi-phasic nature. In addition, the hydroxy metabolites were co-eluted with only one of the test compounds, so they also cannot account for the bi-phasic nature, although they may be causing enhancement or suppression of the mass response.

When modelling of the depletion, Akaike Information Criterion performed adequately in determining which of the mono- and bi-exponential models was the most suitable for the majority of the compounds of this set of test compounds. However, limitations of the AIC make it more suitable for larger data sets and this could be a problem for rapidly metabolised compounds. The corrected CL_{int} values obtained from the bi-exponential model corresponded well to the values calculated from the mono-exponential model from the first phase; however the bi-exponential model is objective and includes all data points which makes it more robust and less prone to uncertainty in the data. The impact of making the *in vivo* predictions from CL_{int} values produced from the mono-exponential model for the first phase or all data points was small for most compounds, although not for all. When the predictions were calculated from the CL_{int} values produced from the bi-exponential model they corresponded well to the predictions from the first phase but provided objectivity. The predictions were closer to the experimental *in vivo* data but with data for only three compounds no conclusions could be drawn about how well they correspond to the data.

The true zero had on average a 20% higher response than 0.5 min time point, but fell very well into the regression line of the models and so did not have a significant impact of the calculated CL_{int} value. For the bi-phasic compounds fit to the bi-exponential model, the CL_{int} values including and excluding the zero time points were very similar, although there is a small risk for a slight under prediction when excluding the zero time point. For compounds with linear depletion, the inclusion or exclusion of the zero point had no impact on the calculated CL_{int} value.

Overall, the quality of the assay was improved and some of the possible mechanisms that could contribute to the bi-phasic depletion behaviour could be ruled out. An unbiased method for determining a CL_{int} value for bi-phasic compounds less prone to under prediction was developed, although further studies have to be performed to fully understand the bi-phasic nature.

6. Future Studies

This project only focused on carboxylic acids although it could be of interest to consider other types of compounds with bi-phasic depletion. By testing additional acids, bases, and neutral compounds, the mechanisms that produce the bi-phasic depletion profile could be investigated. In this project some of the metabolites were identified, although the focus of this project was not to indentify all of the metabolites formed in the reactions. However, full identification of all the metabolites may provide additional information about the bi-phasic nature. A correlation was made between change in shape of the depletion curves at different concentrations and the lipophilicity, although the nonspecific binding of the lipophilic test compounds to the matrix could only be assumed. To fully determine the extent of nonspecific binding an experiment that measures the binding would be beneficial.

It would also be relevant to perform experiments with the medium depletion method, as this could assess if the uptake rate could be a rate limiting factor for the metabolism and hence have an impact on the shape of the depletion curves for this set of test compounds (Jigorel and Houston 2012). In addition, experiments with inhibitors to identify active enzymes during the metabolism of the compounds and any metabolite inhibition would be of interest. It would be relevant to investigate if the change in kinetics of the decay could be due to a change of enzymes catalysing the metabolic reactions during the incubation. If there is a change of metabolising enzymes, the bi-exponential model could be appropriate from a physical point of view.

7. Bibliography

Austin, R. P., et al. (2002). "The influence of nonspecific microsomal binding on apparent intrinsic clearance, and its prediction from physicochemical properties." Drug Metabolism and Disposition **30**(12): 1497-1503.

Austin, R. P., et al. (2005). "The binding of drugs to hepatocytes and its relationship to physicochemical properties." Drug Metabolism and Disposition **33**(3): 419-425.

Baranczewski, P., et al. (2006). "Introduction to in vitro estimation of metabolic stability and drug interactions of new chemical entities in drug discovery and development." Pharmacol Rep **58**(4): 453-472.

Bleicher, K. H., et al. (2003). "Hit and lead generation: beyond high-throughput screening." Nature Reviews Drug Discovery **2**(5): 369-378.

Brandon, E. F., et al. (2003). "An update on in vitro test methods in human hepatic drug biotransformation research: pros and cons." Toxicology and applied pharmacology **189**(3): 233-246.

Chiu, S.-H. L. (1993). "The use of in vitro metabolism studies in the understanding of new drugs." Journal of pharmacological and toxicological methods **29**(2): 77-83.

Clarke, S. (1998). "In vitro assessment of human cytochrome P450." Xenobiotica **28**(12): 1167-1202.

Crespi, C. L. (1995). "Xenobiotic-metabolizing human cells as tools for pharmacological and toxicological research." Advances in drug research **26**: 179-235.

Easterbrook, J., et al. (2001). "Effects of organic solvents on the activities of cytochrome P450 isoforms, UDP-dependent glucuronyl transferase, and phenol sulfotransferase in human hepatocytes." Drug Metabolism and Disposition **29**(2): 141-144.

Hallifax, D., et al. (2010). "Prediction of human metabolic clearance from in vitro systems: retrospective analysis and prospective view." Pharmaceutical research **27**(10): 2150-2161.

Hasler, J. A., et al. (1999). "Human cytochromes P450." Molecular Aspects of Medicine **20**(1): 1-137.

Hewitt, N. J., et al. (2007). "Primary hepatocytes: current understanding of the regulation of metabolic enzymes and transporter proteins, and pharmaceutical practice for the use of hepatocytes in metabolism, enzyme induction, transporter, clearance, and hepatotoxicity studies." Drug metabolism reviews **39**(1): 159-234.

Ichinose, R. and N. Kurihara (1985). "Uptake of dieldrin, lindane, and DDT by isolated rat hepatocytes." Pesticide biochemistry and physiology **23**(1): 116-122.

Jenkins, K. M., et al. (2004). "Automated high throughput ADME assays for metabolic stability and cytochrome P450 inhibition profiling of combinatorial libraries." Journal of pharmaceutical and biomedical analysis **34**(5): 989-1004.

Jigorel, E. and J. B. Houston (2012). "Utility of drug depletion-time profiles in isolated hepatocytes for accessing hepatic uptake clearance: identifying rate-limiting steps and role of passive processes." Drug Metabolism and Disposition **40**(8): 1596-1602.

Jones, H. M. and J. B. Houston (2004). "Substrate depletion approach for determining in vitro metabolic clearance: time dependencies in hepatocyte and microsomal incubations." Drug Metabolism and Disposition **32**(9): 973-982.

Kalvass, J. C., et al. (2001). "Influence of microsomal concentration on apparent intrinsic clearance: implications for scaling in vitro data." Drug Metabolism and Disposition **29**(10): 1332-1336.

Kola, I. and J. Landis (2004). "Can the pharmaceutical industry reduce attrition rates?" Nature Reviews Drug Discovery **3**(8): 711-716.

Li, D., et al. (2010). "Effect of regular organic solvents on cytochrome P450-mediated metabolic activities in rat liver microsomes." Drug Metabolism and Disposition **38**(11): 1922-1925.

Motulsky, H. and A. Christopoulos (2004). Fitting models to biological data using linear and nonlinear regression: a practical guide to curve fitting, Oxford University Press.

Obach, R. S. (1999). "Prediction of human clearance of twenty-nine drugs from hepatic microsomal intrinsic clearance data: an examination of in vitro half-life approach and nonspecific binding to microsomes." Drug Metabolism and Disposition **27**(11): 1350-1359.

Parkinson, A. (2001). Biotransformation of xenobiotics, McGraw-Hill New York.

Plant, N. (2004). "Strategies for using in vitro screens in drug metabolism." Drug discovery today **9**(7): 328-336.

Rendic, S. (2002). "Summary of information on human CYP enzymes: human P450 metabolism data." Drug metabolism reviews **34**(1-2): 83-448.

Riley, R. J. and K. Grime (2004). "Metabolic screening in vitro: metabolic stability, CYP inhibition and induction." Drug Discovery Today: Technologies **1**(4): 365-372.

Smith, D. A., et al. (1996). "Design of drugs involving the concepts and theories of drug metabolism and pharmacokinetics." Medicinal Research Reviews **16**(3): 243-266.

Sohlenius-Sternbeck, A.-K., et al. (2012). "Practical use of the regression offset approach for the prediction of in vivo intrinsic clearance from hepatocytes." Xenobiotica **42**(9): 841-853.

Taavitsainen, P., et al. (2001). "In vitro inhibition of cytochrome P450 enzymes in human liver microsomes by a potent CYP2A6 inhibitor, trans-2-phenylcyclopropylamine

(tranylcypromine), and its nonamine analog, cyclopropylbenzene." Drug Metabolism and Disposition **29**(3): 217-222.

Thompson, T. N. (2001). "Optimization of metabolic stability as a goal of modern drug design." Medicinal Research Reviews **21**(5): 412-449.

Trufelli, H., et al. (2011). "An overview of matrix effects in liquid chromatography–mass spectrometry." Mass spectrometry reviews **30**(3): 491-509.

Tukey, R. H. and C. P. Strassburg (2000). "Human UDP-glucuronosyltransferases: metabolism, expression, and disease." Annual review of pharmacology and toxicology **40**(1): 581-616.

Venkatakrishnan, K., et al. (2003). "Drug metabolism and drug interactions: application and clinical value of in vitro models." Current drug metabolism **4**(5): 423-459.

Wilson, Z., et al. (2003). "Inter-individual variability in levels of human microsomal protein and hepatocellularity per gram of liver." British journal of clinical pharmacology **56**(4): 433-440.

Xue, Y. J., et al. (2008). "Optimization to eliminate the interference of migration isomers for measuring 1-O-β-acyl glucuronide without extensive chromatographic separation." Rapid Communications in Mass Spectrometry **22**(2): 109-120.

8. Appendix I

Table 8. Predictions of *in vivo* plasma clearance using the mono-exponential model fit to all data points as well as the first phase. The table also includes the predicted *in vivo* clearance using the bi-exponential model. No values were generated for Lumiracoxib and Zomepirac from the bi-exponential model.

Predicted plasma clearance CL_H (ml/min/kg)				
	Mono-exponential model		**Bi-exponential model**	***In vivo* data**
	All data points	**First Phase**		
AZ_01	1.1	3.7	3.9	
AZ_02	2.3	8.2	5.8	
AZ_03	1.2	4.1	4.2	
AZ_04	1.0	4.3	4.2	
AZ_05	2.3	2.7	2.9	
AZ_06	6.7	8.4	8.9	
AZ_07	3.2	4.4	5.2	
AZ_08	2.0	5.8	5.7	
AZ_09	7.8	22.1	23.8	79.6
AZ_10	6.3	13.1	14.8	55.9
AZ_11	3.5	10.9	12.2	
AZ_12	1.3	1.3	1.3	
AZ_13	5.0	17.4	18.9	47.6
AZ_14	2.5	8.5	9.1	
AZ_15	8.7	23.3	25.4	
AZ_16	1.7	2.3	2.8	
AZ_17	6.1	8.8	10.6	
Atorvastatin	18.6	18.7	19.7	
Diclofenac	22.4	27.0	27.0	
Flufenamic	5.6	6.2	7.7	
Furosemide	5.1	5.8	5.6	
Indomethacin	0.9	1.0	1.3	
Indoprofen	2.1	2.1	0.7	
Lumiracoxib	16.8	23.8		
Telmisartan	2.0	2.7	2.2	
Zomepirac	0.8	0.8		